

# **Steel 8615 Axial Case-Core Deep CD Iteration #161 / #162**

## **Monotonic Tensile and Fatigue Test Results Including Overload Tests**

Prepared by:

Changjian Wei

and

Hong-Tae Kang

Department of Mechanical Engineering  
College of Engineering and Computer Science  
The University of Michigan-Dearborn  
Dearborn, Michigan 48128

Prepared for:

The AISI Bar Steel Applications Group

May 2016



American Iron and Steel Institute  
2000 Town Center, Suite 320  
Southfield, Michigan 48075  
tel: 248-945-4777  
fax: 248-352-1740

[www.autosteel.org](http://www.autosteel.org)

# TABLE OF CONTENTS

<b>SUMMARY .....</b>	<b>1</b>
<b>I. EXPERIMENTAL PROGRAM.....</b>	<b>2</b>
1.1 Material and Specimen Fabrication .....	2
1.1.1 Material .....	2
1.1.2 Specimen.....	2
1.2 Testing Equipment .....	3
1.2.1 Apparatus .....	3
1.2.2 Alignment.....	3
1.3 Test Methods and Procedures .....	4
1.3.1 Monotonic tension tests .....	4
1.3.2 Constant amplitude fatigue tests .....	4
1.3.3 Periodic overload fatigue tests .....	5
<b>II. EXPERIMENTAL RESULTS AND ANALYSIS .....</b>	<b>7</b>
2.1 Microstructural Data .....	7
2.2 Monotonic Deformation Behavior .....	7
2.3 Cyclic Deformation Behavior .....	9
2.3.1 Transient cyclic response .....	9
2.3.2 Steady-state cyclic deformation .....	9
2.4 Constant Amplitude Fatigue Behavior.....	10
2.5 Periodic Overload Fatigue Behavior.....	12
<b>TABLES.....</b>	<b>14</b>
<b>FIGURES.....</b>	<b>14</b>
<b>REFERENCES.....</b>	<b>30</b>
<b>APPENDIX A .....</b>	<b>31</b>
<b>APPENDIX B .....</b>	<b>43</b>
<b>APPENDIX C .....</b>	<b>45</b>

## NOMENCLATURE

$A_o, A_f$	initial, final area	S	engineering stress
HB, HRB, HRC	Brinell, Rockwell B-Scale, Rockwell C-Scale Hardness Number	YS, UYS, LYS, YS'	monotonic yield, upper yield, lower yield, cyclic yield strength
b, c, n	fatigue strength, fatigue ductility, strain hardening exponent	YPE	yield point elongation
$D_o, D_f$	initial, final diameter	$S_u$	ultimate tensile strength
e	engineering strain	EL%	percent elongation
E, E'	monotonic, cyclic strength coefficient	RA%	percent reduction in area
K, K'	monotonic, cyclic strength coefficient	$\sigma, \sigma_f, \sigma_f'$	true stress, true fracture strength, fatigue strength coefficient
$L_o, L_f$	initial, final gage length	$\epsilon_e, \epsilon_p, \epsilon$	true elastic, plastic, total strain
$N_{50\%}, (N_f)_{10\%},$ $(N_f)_{50\%}$	number of cycles to midlife, 10% load drop, 50% load drop	$\epsilon_f, \epsilon_f'$	true fracture ductility, fatigue ductility coefficient
$P_f, P_u$	fracture, ultimate load	$\epsilon_a, \epsilon_m, \Delta\epsilon$	strain amplitude, mean strain, strain range
R	strain ratio	$\Delta\epsilon_e, \Delta\epsilon_p$	elastic, plastic strain range

## UNIT CONVERSION TABLE

---

<u>Measure</u>	<u>SI Unit</u>	<u>US Unit</u>	<u>From SI to US</u>	<u>From US to SI</u>
Length	mm	in	1 mm = 0.03937 in	1 in = 25.4 mm
Area	mm <sup>2</sup>	in <sup>2</sup>	1 mm <sup>2</sup> = 0.00155 in <sup>2</sup>	1 in <sup>2</sup> = 645.16 mm <sup>2</sup>
Load	kN	klb	1kN = 0.2248 klb	1 klb = 4.448 kN
Stress	MPa	ksi	1 MPa = 0.14503	1 ksi = 6.895 MPa
Temperature	°C	°F	°C = (°F - 32) /1.8	°F = (°C * 1.8) + 32

---

In SI Unit

1 kN = 10<sup>3</sup> N    1 Pa = 1 N/m<sup>2</sup>    1 MPa = 10<sup>6</sup> Pa = 1 N/mm<sup>2</sup>    1 GPa = 10<sup>9</sup> Pa

In US Unit

1 klb = 10<sup>3</sup> lb    1 psi = 1 lb/in<sup>2</sup>    1 ksi = 10<sup>3</sup> psi

---

## **SUMMARY**

Monotonic tensile properties and fatigue behavior data were obtained for steel material of iteration 161. Periodic overload behavior data were obtained for iteration 162. The material was provided by AISI. Two tensile tests were performed to acquire the desired monotonic properties. Both tests gave similar results. Thirteen constant amplitude strain-controlled fatigue tests at six strain levels were performed to obtain the fatigue life and cyclic deformation curves and properties. The experimental procedure followed and results obtained are presented and discussed in this report. Periodic overload fatigue behavior and data were also obtained from four strain-controlled periodic overload fatigue tests. The experimental procedure followed and results obtained from periodic overload tests are also presented and discussed in this report.

# **I. EXPERIMENTAL PROGRAM**

## **1.1 Material and Specimen Fabrication**

### **1.1.1 Material**

The steel material was provided by AISI. The test specimen was prepared from an 8615 Axial steel grade with the condition of carburized core with deep case (case depth = 10% of gage diameter). Inclusion distribution and microstructure of the material in case area are shown in Figure 1, and inclusion distribution and microstructure in core area are shown in Figure 2. The hardness of this material in gauge and grip are 35 HRC and 25 HRC, respectively (see Appendix B).

### **1.1.2 Specimen**

In this study, identical round specimens were used for monotonic and fatigue tests. The specimen configuration and dimensions are shown in Figure 1. This configuration deviates slightly from the specimens recommended by ASTM Standard E606 [1]. The recommended specimens have uniform gage sections. The specimen geometry shown in Figure 3 differs by using a large secondary radius in the gage section to compensate for the slight stress concentration at the gage to grip section transition.

All specimens were provided by AISI. Heat treatment and Machining were needed at first. The specimens were then polished prior to testing. All remaining polishing marks coincided with the longitudinal direction of the specimen. The polished surfaces were carefully examined under magnification to ensure complete removal of the machine marks within the test section. Test specimens were protected immediately after machining and polishing until they were tested, since they may be susceptible to corrosion in moist room- temperature air.

Before testing, the measurement of each specimen was needed. The measured dimensions are shown in Table A.3. Imprint specimen numbers on both ends of the test section in regions of low stress, away from grip contact surfaces.

## **1.2 Testing Equipment**

### **1.2.1 Apparatus**

A MTS 810 Material Test System which included a closed-loop servo-controlled hydraulic axial load frame was used to conduct both monotonic and fatigue tests. The load cell used had a capacity of 100 kN. The MTS 646 Hydraulic Collet Grips with 0.50 in (12.7mm) diameter collets were employed to secure the specimens' ends in series with the load cell.

Total strain was controlled and measured using an extensometer rated as ASTM class B1 [2]. Here in this study, MTS Model 632.26E-20 Extensometer was chosen. The calibration of the extensometer was verified by the professional of the MTS. The extensometer had a gage length of 0.30 in and was capable of measuring strains up to 15%.

In order to protect the specimens' surface from the knife-edges of the extensometer, ASTM Standard E606 recommends the use of transparent tape or epoxy to 'cushion' the attachment. For this study, it was found that the application of transparent tape strips was difficult due to the size of the test section. Therefore, epoxy was considered to be the best protection. The tests were performed using M-coat A. Prior to the testing, made marks on both side of each specimen's gage length where the knife-edges of the extensometer can be set up. After each specimen was broken, observe the failure location and see if it is inside the gage length.

### **1.2.2 Alignment**

Alignment of the load path components was essential for the accurate measurement of strain-life material constants. Significant effort was put forth to align the load path components (such as load cell, grips, specimens, and actuator). Misalignment can result from both tilt and offset between the central line of the load train components. The alignment was done by the professional of the MTS in accordance with ASTM Standard E1012 [3].

## **1.3 Test Methods and Procedures**

### **1.3.1 Monotonic tension tests**

Monotonic tests in this study were performed using test methods specified by ASTM Standard E8 [4]. Two specimens were used to obtain the monotonic properties.

In order to protect the extensometer, strain control was used up to 10% strain, until the point of ultimate tensile strength had been crossed. After this point, displacement control was used until fracture. MTS 793.00 System Software and MTS 793.10 MultiPurpose Testware were used for the monotonic tests. The specimens are tested to fracture under strain or displacement control. For the elastic and initial yield region (0% to 0.5% strain) as well as the period up to which the extensometer was removed, a strain rate of 0.0025 in/in/min (0.001 mm/mm/s) was chosen. This strain rate was three-quarters of the maximum allowable rate specified by ASTM Standard E8 for the initial yield region. After the extensometer was removed, a displacement rate of 0.006 in/min (0.00254 mm/s) was used.

After the tension tests were concluded, the broken specimens were carefully reassembled. The final gage lengths of the fractured specimens, the final diameter, and the necking radius were then measured by a digital caliper for several times to make sure that the results were accurate. It should be noted that prior to the test, the initial diameter was measured with this same instrument.

### **1.3.2 Constant amplitude fatigue tests**

Constant-amplitude axial fatigue tests provide information about the cyclic and fatigue behavior of materials. All constant amplitude fatigue tests in this study were performed according to ASTM Standard E606. It is recommended by this standard that at least 10 specimens be used to generate the fatigue properties. For this study, 13 specimens at 6 different strain amplitudes ranging from 0.300% to 0.800% were utilized. MTS 793.00 System Software and MTS 793.10 MultiPurpose Testware were used in all strain-controlled tests. During each strain-controlled test, the total strain was recorded using the extensometer output. Test data were automatically recorded



throughout each test.

There were two control modes used for these tests. Strain control was used in all tests with plastic deformation. For one of the elastic tests, strain control was used initially to determine the stabilized load, then load control was used for the remainder of the test and for the rest of the elastic tests, load control was used throughout. One reason for the change in control mode was due to the frequency limitation on the extensometer. Besides, at long lives, the total strain becomes quite small and the control of these quantities requires accurate instrumentation and extreme precision in the test procedure. Tests with anticipated lives exceeding 1 million cycles are change to load control mode when the load are stabilized. For the strain-controlled test, the applied frequencies ranged from 0.3 Hz to 1.0Hz in order to keep a strain rate about 0.02 in/in/sec. For the load-controlled tests, load waveforms with frequencies of up to 20Hz were used in order to shorten the overall test duration. All tests were conducted using a triangular waveform.

Failure of the specimens is defined when the maximum load decreases by 50% because of a crack or cracks being present. The strain-life curve is developed over a range of approximately 100 to 5,000,000 cycles (10,000,000 reversals).

### **1.3.3 Periodic overload fatigue tests**

The overload tests were conducted to investigate the effects of periodic overloads on the fatigue life of smaller subsequent cycles. For this study, 4 specimens were tested at 4 different strain amplitudes. The periodic overload tests were run in strain-control with MTS 793.10 MultiPurpose Testware. During each strain-controlled test, the total strain was recorded using the extensometer output. Test data were automatically recorded throughout each test.

The input signal consisted of a periodic fully reversed overload of the type shown in Figure 13. The load history in these tests consisted of repeated load blocks made up of one fully-reversed overload cycle followed by a group of smaller constant amplitude cycles having the same maximum stress as the overload cycle. The overload cycles were applied at frequent intervals to maintain a low crack opening stress resulting in

the subsequent cycles being fully open.

With this overload history, as the large cycles become more frequent, the fraction of the total damage done by them increases and that done by the small cycles decreases. The fully reversed strain amplitude for the overload cycle corresponded to  $10^4$  cycles to failure. The number of small cycles per block,  $N_{SC}$  was adjusted so that they cause 80 to 90% of the damage per block. Small cycle strain levels were selected at or below the run out level of the constant amplitude tests. Small cycles strain amplitudes were used from 0.315% to 0.250% and the number of small cycles per overload cycle was 100.

## II. EXPERIMENTAL RESULTS AND ANALYSIS

### 2.1 Microstructural Data

A specimen was sectioned longitudinally from the grip end and transversely from the gage section to obtain a general microstructure description. The sample was prepared with standard test procedures for sectioning, mounting, polishing, and etched. The sample was reviewed and observed under a microscope. The microphotographs revealed the microstructure of the material. Figure 1 shows a high magnification photograph of the inclusion distribution and microstructure in the case area, and Figure 2 shows a high magnification photograph of the inclusion distribution and microstructure from the core area. Both of the figures were provided by Chrysler. The chemistry of the material is presented in Table 1.

### 2.2 Monotonic Deformation Behavior

The properties determined from monotonic tensile tests were the following: modulus of elasticity (E), yield strength (YS), ultimate tensile strength ( $S_u$ ), percent elongation (%EL), percent reduction in area (%RA), true fracture strength ( $\sigma_f$ ), true fracture ductility ( $\epsilon_f$ ), strength coefficient (K), and strain hardening exponent (n).

True stress ( $\sigma$ ), true strain ( $\epsilon$ ), and true plastic strain ( $\epsilon_p$ ) were calculated from engineering stress (S) and engineering strain (e), according to the following relationships which are based on constant volume assumption:

$$\sigma = S(1 + e) \quad (1a)$$

$$\epsilon = \ln(1 + e) \quad (1b)$$

$$\epsilon_p = \epsilon - \epsilon_e = \epsilon - \frac{\sigma}{E} \quad (1c)$$

The true stress ( $\sigma$ ) - true strain ( $\epsilon$ ) plot is often represented by the Ramberg - Osgood equation:

$$\epsilon = \epsilon_e + \epsilon_p = \frac{\sigma}{E} + \left(\frac{\sigma}{K}\right)^{\frac{1}{n}} \quad (2)$$

The strength coefficient,  $K$ , and strain hardening exponent,  $n$ , are the intercept and slope of the best line fit to true stress ( $\sigma$ ) versus true plastic strain ( $\epsilon_p$ ) data in log-log scale:

$$\sigma = K(\epsilon_p)^n \quad (3)$$

In accordance with ASTM Standard E739 [5], when performing the least squares fit, the true plastic strain ( $\epsilon_p$ ) was the independent variable and the true stress ( $\sigma$ ) was the dependent variable. These plots for the two tests conducted are shown in Figure 4. As can be seen from this figure, the two curves are very close to each other. To generate the  $K$  and  $n$  values, the range of data used in this figure was chosen according to the definition of discontinuous yielding specified in ASTM Standard E646 [6]. Therefore, the valid data range occurred between the end of yield point extension and the strain at maximum load.

The true fracture strength was corrected for necking according to the Bridgman correction factor [7]:

$$\sigma_f = \frac{\frac{P_f}{A_f}}{\left[1 + \frac{4R}{D_f}\right] \ln\left[1 + \frac{D_f}{4R}\right]} \quad (4)$$

where  $P_f$  is load at fracture,  $R$  is the neck radius, and  $D_f$  is the diameter at fracture.

The true fracture ductility,  $\epsilon_f$ , was calculated from the relationship based on constant volume:

$$\epsilon_f = \ln\left(\frac{A_0}{A_f}\right) = \ln\left(\frac{1}{1-RA}\right) \quad (5)$$

where  $A_f$  is the cross-sectional area at fracture,  $A_0$  is the original cross-sectional area, and  $RA$  is the reduction in area.

A summary of the monotonic properties for this material is provided in Table A.1. The monotonic stress-strain curves are shown in Figure 5. As can be seen from this figure, the two curves are very close to each other. Refer to Table A.1 for a summary of the monotonic test results.

## 2.3 Cyclic Deformation Behavior

### 2.3.1 Transient cyclic response

Transient cyclic response describes the process of cyclic-induced change in deformation resistance of a material. Data obtained from constant amplitude strain-controlled fatigue tests were used to determine this response. Plots of stress amplitude variation versus applied number of cycles can indicate the degree of transient cyclic softening/hardening. Also, these plots show when cyclic stabilization occurs. A composite plot of the transient cyclic response for the steel studied is shown in Figure A.1. The transient response was normalized on the rectangular plot in Figure A.1a, while a semi-log plot is shown in Figure A.1b. Even though multiple tests were conducted at each strain amplitude, data from one test at each strain amplitude tested are shown in these plots.

### 2.3.2 Steady-state cyclic deformation

Another cyclic behavior of interest was the steady state or stable response. Data obtained from constant amplitude strain-controlled fatigue tests were also used to determine this response. The properties determined from the steady-state hysteresis loops were the following: cyclic modulus of elasticity ( $E'$ ), cyclic strength coefficient ( $K'$ ), cyclic strain hardening exponent ( $n'$ ), and cyclic yield strength ( $YS'$ ). Half-life (midlife) hysteresis loops and data were used to obtain the stable cyclic properties.

Similar to monotonic behavior, the cyclic true stress-strain behavior can be characterized by Ramberg-Osgood type equation:

$$\frac{\Delta\varepsilon}{2} = \frac{\Delta\varepsilon_e}{2} + \frac{\Delta\varepsilon_p}{2} = \frac{\Delta\sigma}{2E} + \left(\frac{\Delta\sigma}{2K'}\right)^{\frac{1}{n'}} \quad (6)$$

It should be noted that in Equation 6 and the other equations that follow,  $E$  is the average modulus of elasticity that was calculated from the monotonic tests.

The cyclic strength coefficient,  $K'$ , and cyclic strain hardening exponent,  $n'$ , are the intercept and slope of the best line fit to true stress amplitude ( $\Delta\sigma/2$ ) versus true plastic strain amplitude ( $\Delta\varepsilon_p/2$ ) data in log-log scale:

$$\frac{\Delta\sigma}{2} = K' \left( \frac{\Delta\varepsilon_p}{2} \right)^{n'} \quad (7)$$

In accordance with ASTM Standard E739 [5], when performing the least squares fit, the true plastic strain amplitude ( $\Delta\varepsilon_p/2$ ) was the independent variable and the stress amplitude ( $\Delta\sigma/2$ ) was the dependent variable. The true plastic strain amplitude was calculated by the following equation:

$$\frac{\Delta\varepsilon_p}{2} = \frac{\Delta\varepsilon}{2} - \frac{\Delta\sigma}{2E} \quad (8)$$

This plot is shown in Figure 6. To generate the  $K'$  and  $n'$  values, the range of data used in this figure was chosen for  $\left[ \frac{\Delta\varepsilon_p}{2} \right]_{calculated} \geq 0.001$  in/in.

The cyclic stress-strain curve reflects the resistance of a material to cyclic deformation and can be vastly different from the monotonic stress-strain curve. The cyclic stress-strain curve is shown in Figure 7. In Figure 8, superimposed plots of monotonic and cyclic curves are shown. As can be seen in this figure, the material cyclically softened. Figure A.2 shows a composite plot of the steady-state (midlife) hysteresis loops. Even though multiple tests were conducted at each strain amplitude, the stable loops from only one test at each strain amplitude are shown in this plot.

## 2.4 Constant Amplitude Fatigue Behavior

Constant amplitude strain-controlled fatigue tests were performed to determine the strain-life curve. The following equation relates the true strain amplitude to the fatigue life:

$$\frac{\Delta\varepsilon}{2} = \frac{\Delta\varepsilon_e}{2} + \frac{\Delta\varepsilon_p}{2} = \frac{\sigma'_f}{E} (2N_f)^b + \varepsilon'_f (2N_f)^c \quad (9)$$

where  $\sigma'_f$  is the fatigue strength coefficient,  $b$  is the fatigue strength exponent,  $\varepsilon'_f$  is the fatigue ductility coefficient,  $c$  is the fatigue ductility exponent,  $E$  is the monotonic modulus of elasticity, and  $2N_f$  is the number of reversals to failure.

The fatigue strength coefficient,  $\sigma'_f$ , and fatigue strength exponent,  $b$ , are the intercept and slope of the best line fit to true stress amplitude ( $\Delta\sigma/2$ ) versus reversals to failure ( $2N_f$ ) data in log-log scale:

$$\frac{\Delta\sigma}{2} = \sigma'_f(2N_f)^b \quad (10)$$

In accordance with ASTM Standard E739 [5], when performing the least squares fit, the stress amplitude ( $\Delta\sigma/2$ ) was the independent variable and the reversals to failure ( $2N_f$ ) was the dependent variable. This plot is shown in Figure 9. To generate the  $\sigma'_f$  and  $b$  values, all data, with the exception of the run-out tests, in the stress-life figure were used.

The fatigue ductility coefficient,  $\epsilon'_f$ , and fatigue ductility exponent,  $c$ , are the intercept and slope of the best line fit to calculated true plastic strain amplitude ( $\Delta\epsilon_p/2$ ) versus reversals to failure ( $2N_f$ ) data in log-log scale:

$$\left(\frac{\Delta\epsilon_p}{2}\right)_{calculated} = \epsilon'_f(2N_f)^c \quad (11)$$

In accordance with ASTM Standard E739 [5], when performing the least squares fit, the true plastic strain amplitude ( $\Delta\epsilon_p/2$ ) was the independent variable and the reversals to failure ( $2N_f$ ) was the dependent variable. The calculated true plastic strain amplitude was determined from Equation 8. This plot is shown in Figure 10. To generate the  $\epsilon'_f$  and  $c$  values, the range of data used in this figure was chosen for  $\left[\frac{\Delta\epsilon_p}{2}\right]_{calculated} \geq 0.001$  in/in.

The true strain amplitude versus reversals to failure plot is shown in Figure 11. This plot displays the strain-life curve (Eqn. 9), the elastic strain portion (Eqn. 10), the plastic strain portion (Eqn. 11) and superimposed fatigue data. A summary of the cyclic properties for this steel is provided in Table 2. Table A.2 provides the summary of the fatigue test results.

A parameter often used to characterize fatigue behavior at stress concentrations, such as at the root of a notch, is Neuber parameter [7]. Neuber's stress range is given by:

$$\sqrt{(\Delta\epsilon)(\Delta\sigma)E} = 2\sqrt{(\sigma'_f)^2(2N_f)^{2b} + \sigma'_f\epsilon'_fE(2N_f)^{b+c}} \quad (12)$$

A plot of Neuber stress range versus reversals to failure is shown in Figure 12. This figure displays the Neuber curve based on Eqn. 12 and superimposed fatigue data for this material.

## 2.5 Periodic Overload Fatigue Behavior

Periodic Overload strain-controlled fatigue tests were performed to determine the effective strain-life curve. The effective strain-life curve is plotted using the strain amplitude of the small cycles in the overload block and the calculated equivalent life. The equivalent fatigue lives for the smaller cycles were obtained using the linear damage rule:

$$\frac{N_{OL}}{N_{f,OL}} + \frac{N_{SC}}{N_{f,SC(eq)}} = 1 \quad (13)$$

Where  $N_{OL}$  is the number of overload cycles in a periodic overload test,  $N_{f,OL}$  is the number of cycles to failure if only overloads were applied in a test,  $N_{SC}$  is the number of smaller cycles in a periodic overload test, and  $N_{f,SC(eq)}$  is the computed equivalent fatigue life for the smaller cycles.

The linear damage rule was also used to calculate the cumulative damage of the overload cycles,  $D_{OL}$ , as

$$\frac{N_{SC}}{N_{f,SC(eq)}} = 1 \quad (14)$$

Figure 14 shows the effective strain-life data superimposed on the constant amplitude strain life plot. Table A.4 presents a summary of the periodic overload test results.

A plot of the SWT parameter for both the constant amplitude and overload data provides another method of comparison between the two sets of data, where the mean stress present in the small cycles is taken into account. The SWT parameter is given by

$$\sigma_{max}\varepsilon_a = \frac{1}{E} \left[ (\sigma'_f)^2 (2N_f)^{2b} + \sigma'_f \varepsilon'_f E (2N_f)^{b+c} \right] \quad (15)$$

where  $\sigma_{max} = \sigma_m + \sigma_a$ . The SWT plot is shown in Figure 15. As in the constant amplitude strain-life curve, the overload data and effective strain-life curve diverged from the constant amplitude curve.

Plots of the overload cycle and small cycle stress amplitude variation versus applied number of blocks can indicate the degree of transient cyclic soften/hardening. Also, these plots show when cyclic stabilization occurs over the life of the specimen. A composite plot of the small cycle transient cyclic response for the steel studied is shown



in Figure A.3. A composite plot of the overload cycle transient cyclic response is shown in Figure A.4. The amplitude of the transient response is shown in the Figure A.3a and A.4a while the mean of the transient response is shown in Figure A.3b and A.4b. While small cycle stress amplitude was constant during each test (Figure A.3a), there was significant small cycle mean stress relaxation (Figure A.3b).

Stress response of small cycles was also evaluated within a single block. This can be seen in Figure A.5a, which shows the stress amplitude at each strain level within a single block at midlife and in Figure A.5b, which is a plot of the mean stress at each strain level within a single block at midlife. In this study, the #100 block was chosen at each strain amplitude to get the stress values, data from each test are shown in these plots. These plots show steady state stress response within a load block.

The midlife hysteresis loops for each small cycle strain level are shown in Figures A.6a through A.6d. The small cycle loop was taken from the mid-cycle of the midlife block.

**Table 1: Chemical Composition of Steel 8615 (Courtesy of Chrysler)**

<b>Element</b>	<b>Wt.%</b>
Carbon, C	0.110%
Manganese, Mn	0.840%
Phosphorus, P	0.009%
Sulfur, S	0.035%
Silicon, Si	0.300%
Nickel, Ni	0.400%
Chromium, Cr	0.600%
Molybdenum, Mo	0.200%
Copper, Cu	0.140%
Tin, Sn	0.007%
Aluminum, Al	0.030%
Vanadium, V	0.005%
Niobium, Nb	0.002%
Oxygen, O	0.0015%

**Table 2: Summary of the Mechanical Properties**

---

<b>Monotonic Properties</b>	<b>Average</b>	<b>Range</b>
Modulus of elasticity, E, GPa:	206.64	205.24-208.03
Yield strength (0.2% offset), YS, MPa:	1017.03	996.28-1037.78
Ultimate strength, S <sub>u</sub> , MPa:	1182.35	1163.81-1200.89
Percent elongation, %EL (%):	2.81%	2.79%-2.83%
Percent reduction in area, %RA (%):	2.47%	2.47%
Strength coefficient, K, MPa:	4381.85	4025.3-4738.4
Strain hardening exponent, n:	0.2353	0.2256-0.2449
True fracture strength, $\sigma_f$ , MPa:	731.41	712.33-750.48
True fracture ductility, $\epsilon_f$ (%):	2.77%	2.77%

<b>Cyclic Properties</b>	<b>Average</b>	<b>Range</b>
Cyclic modulus of elasticity, E', GPa:	207.62	202.0 – 210.3
Fatigue strength coefficient, $\sigma'_f$ , MPa:	1721.3	-
Fatigue strength exponent, b:	-0.06	-
Fatigue ductility coefficient, $\epsilon'_f$ :	0.0129	-
Fatigue ductility exponent, c:	-0.276	-
Cyclic strength coefficient, K', MPa:	4091.1	-
Cyclic strain hardening exponent, n':	0.2061	-
Cyclic yield strength, YS', MPa:	1138.46	-
Fatigue Limit (defined at 10 <sup>6</sup> cycles), MPa	720.77	-

---

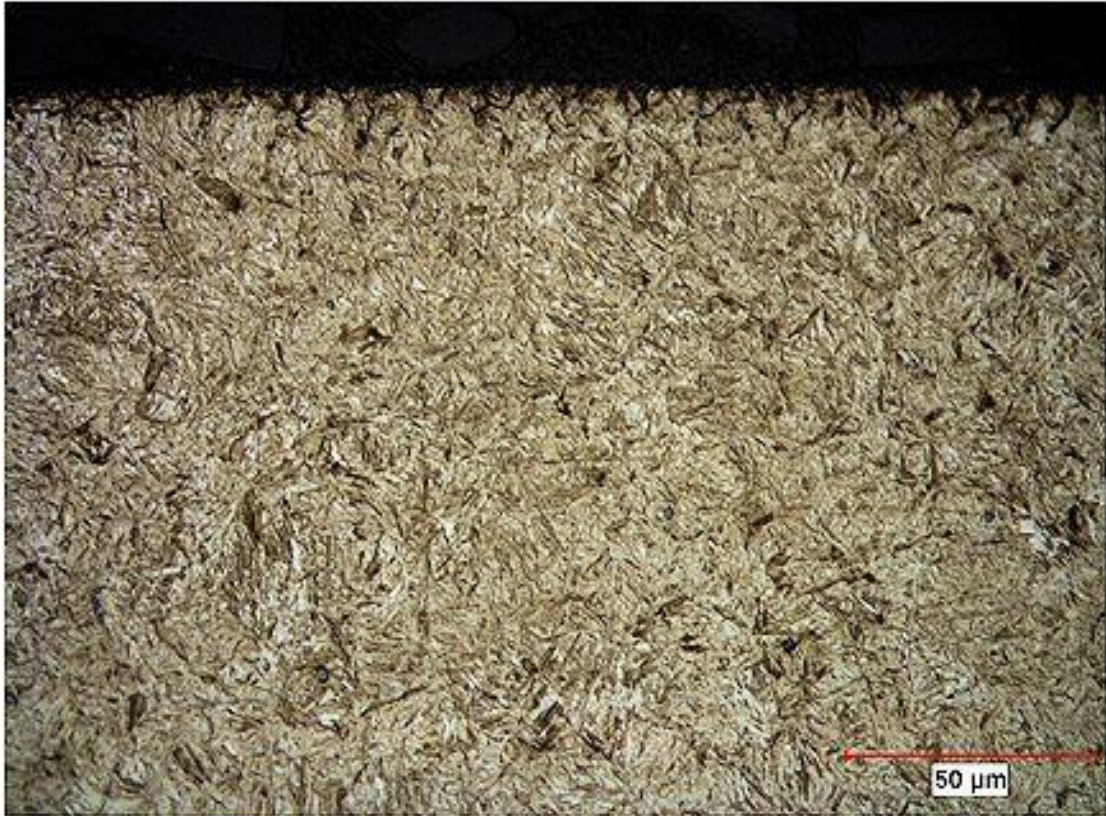


Figure 1: Photograph of the inclusion distribution in the case area (Courtesy of Chrysler)



Figure 2: Photograph of the inclusion distribution in the core area (Courtesy of Chrysler)

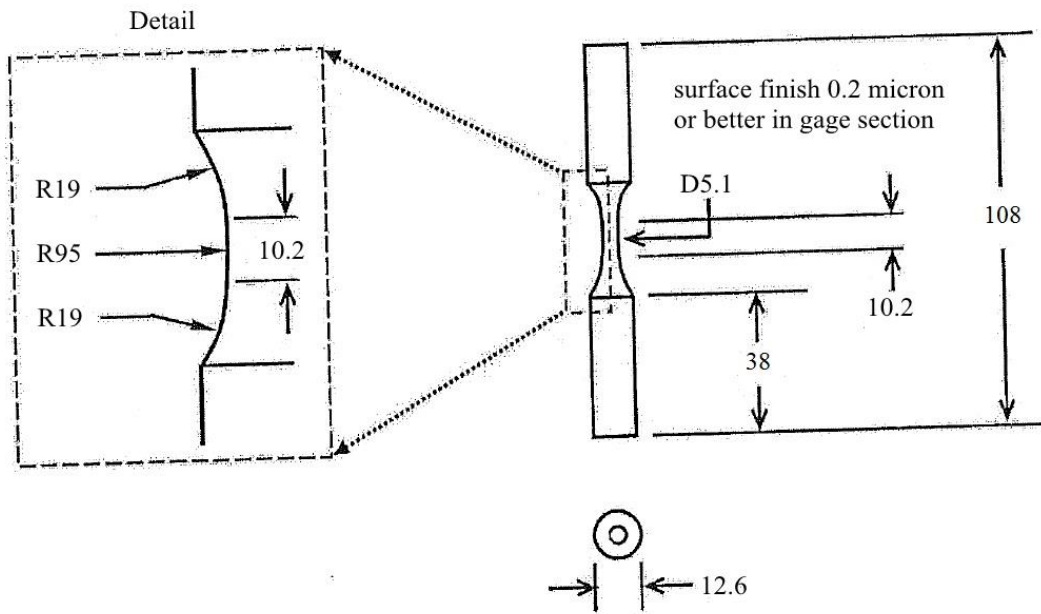


Figure 3: Specimen configuration and dimensions (mm)

## True Stress vs. True Plastic Strain

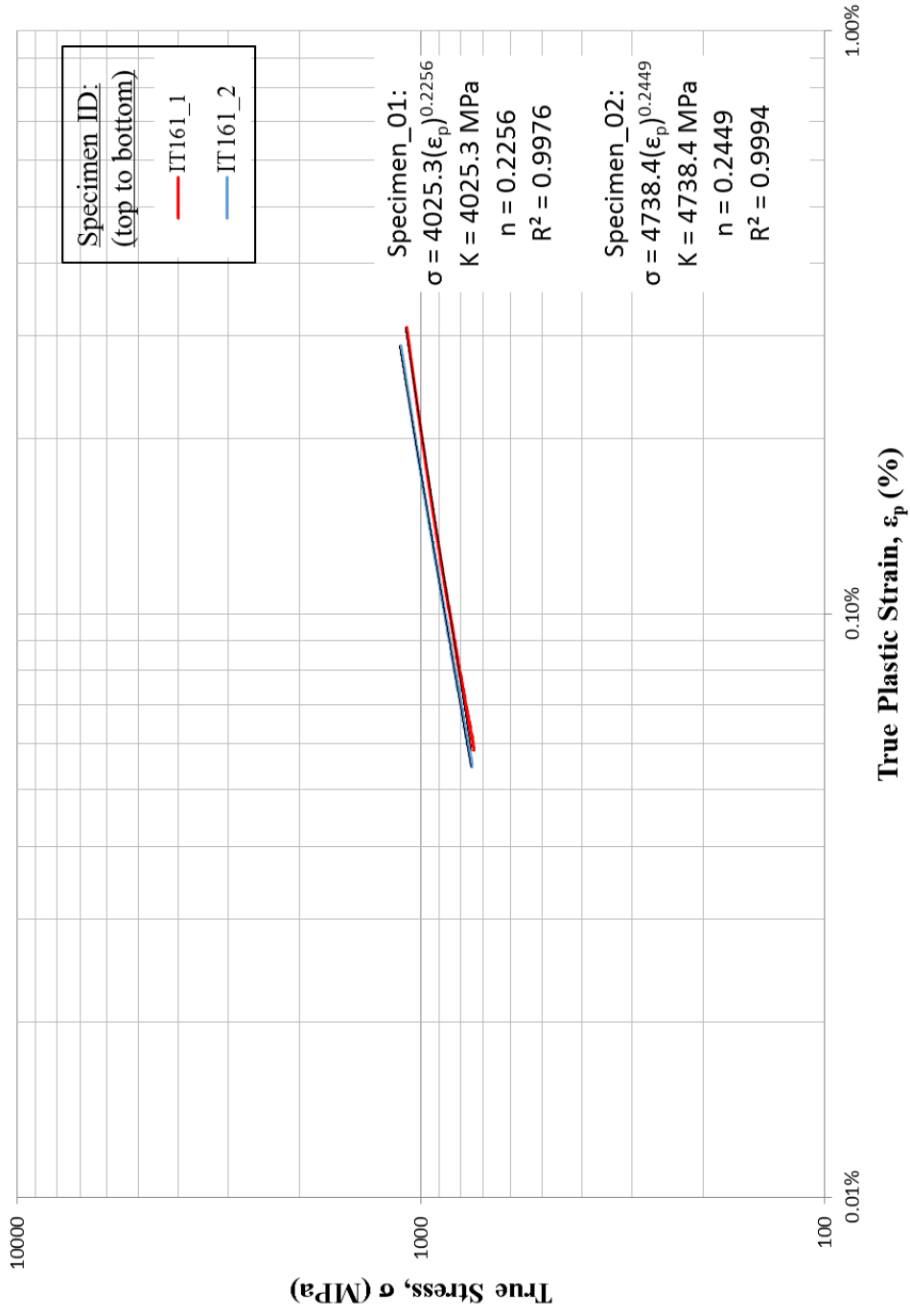


Figure 4: True stress versus true plastic strain



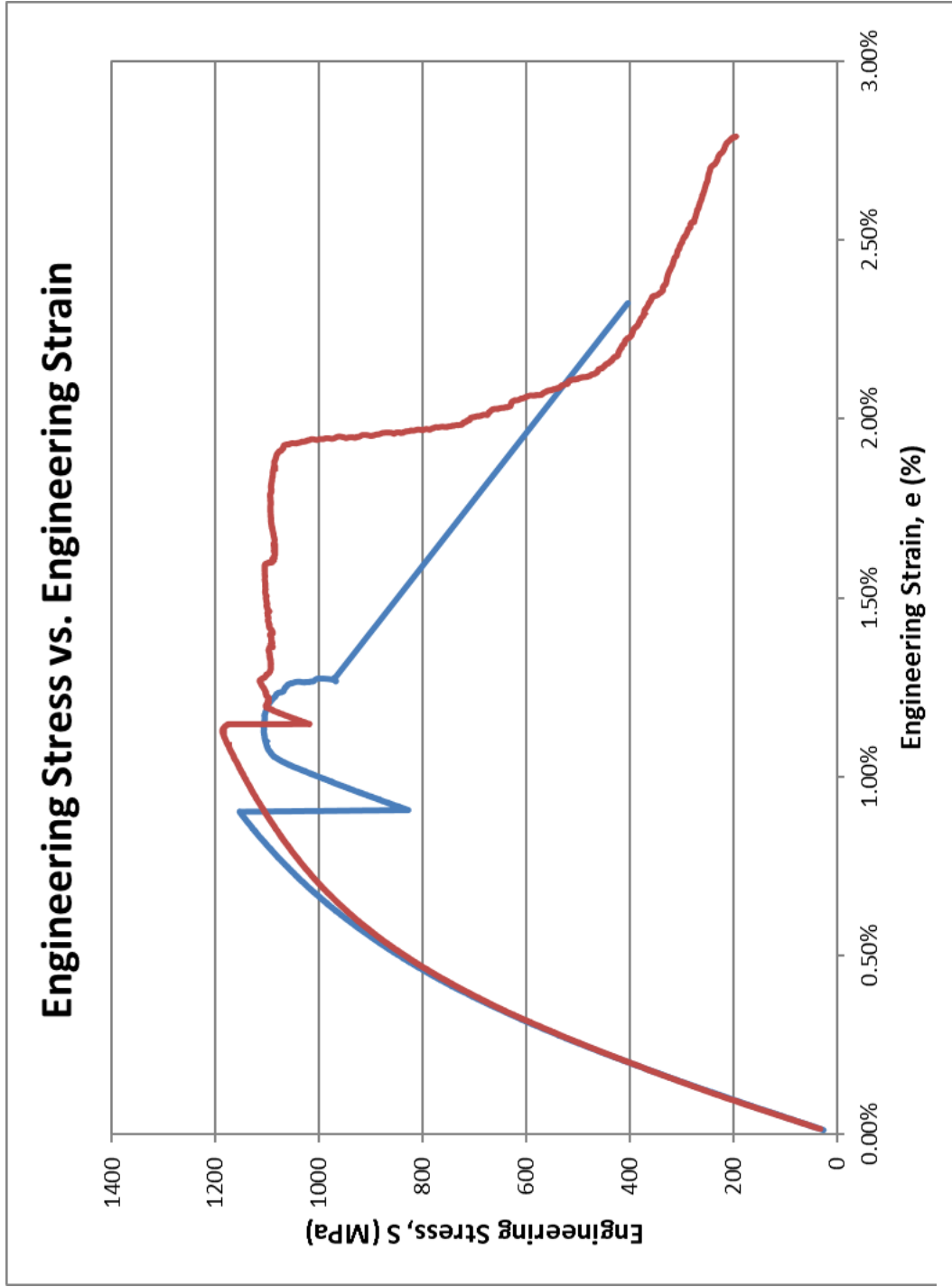


Figure 5: Monotonic stress-strain curves

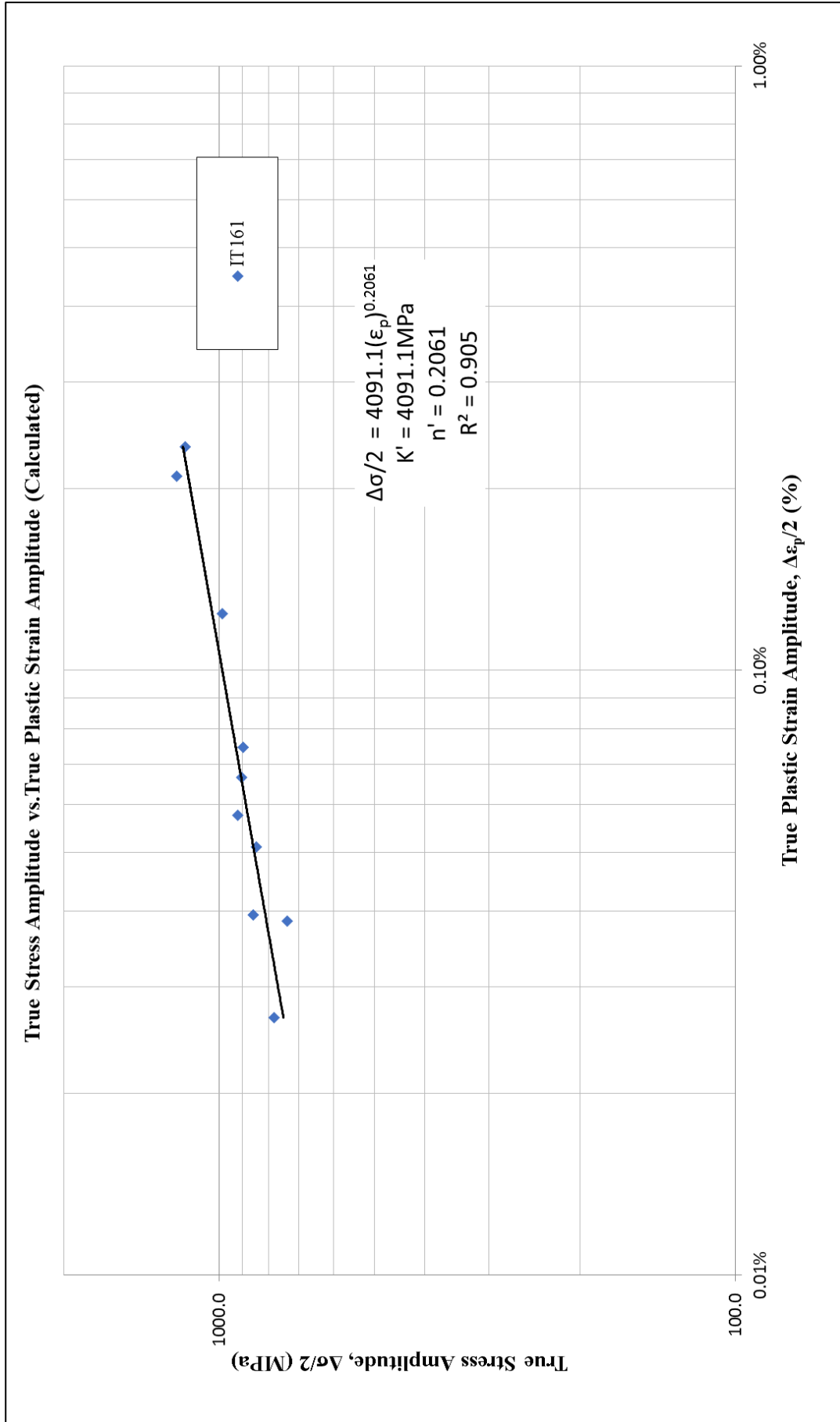


Figure 6: True stress amplitude versus true plastic strain amplitude (calculated)



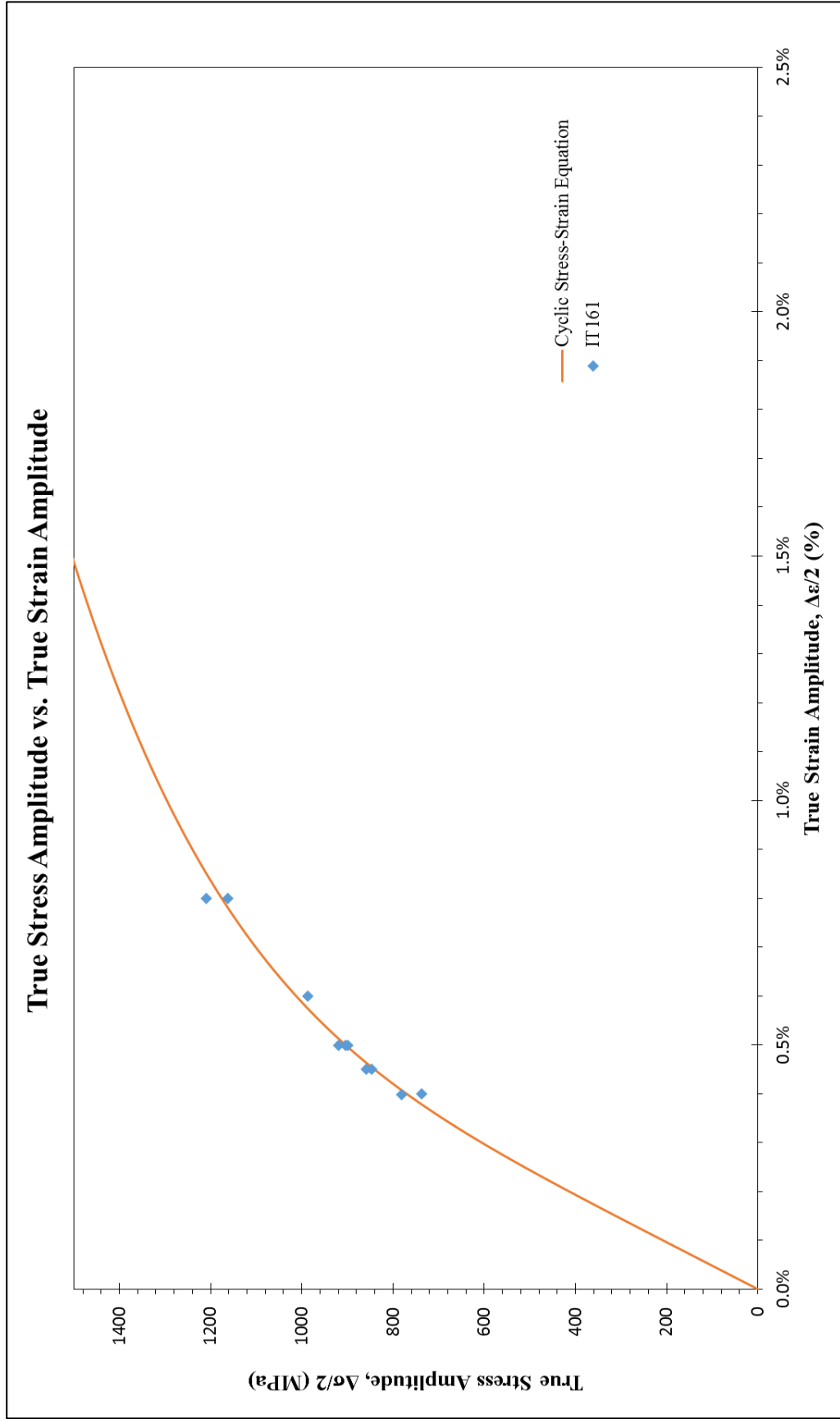


Figure 7: True stress amplitude versus true strain amplitude

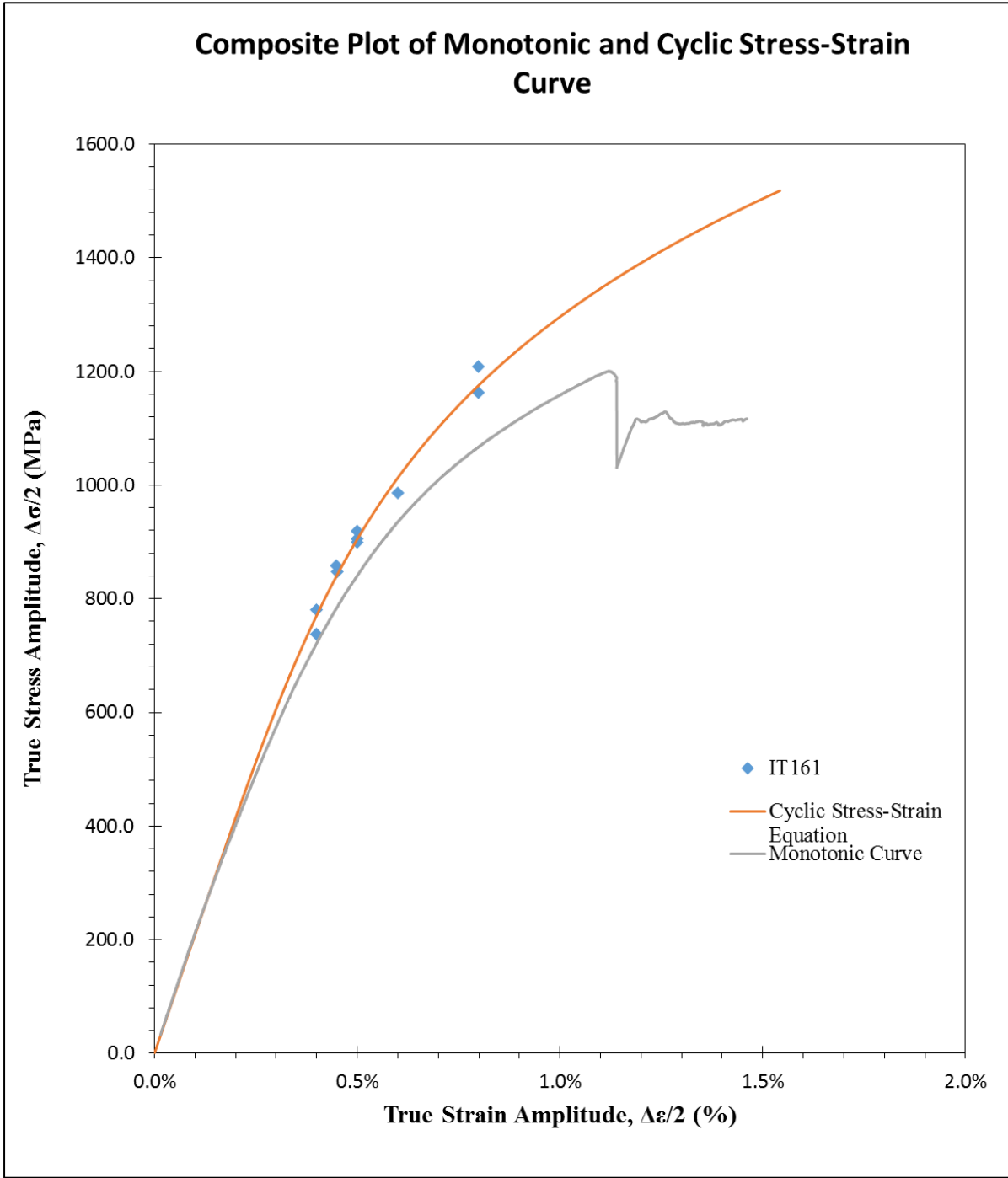


Figure 8: Composite plot of cyclic and monotonic stress-strain curves

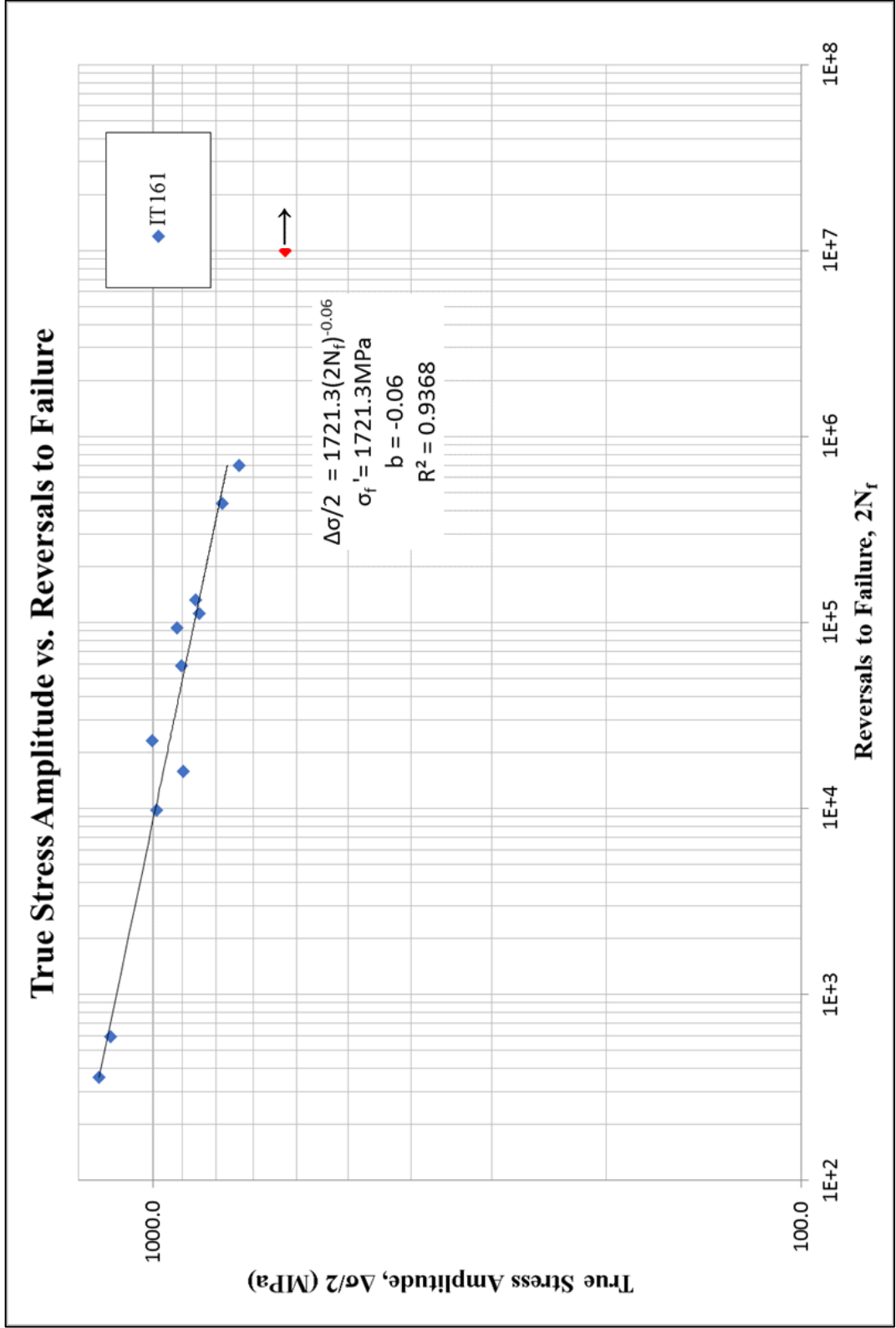


Figure 9: True stress amplitude versus reversals to failure

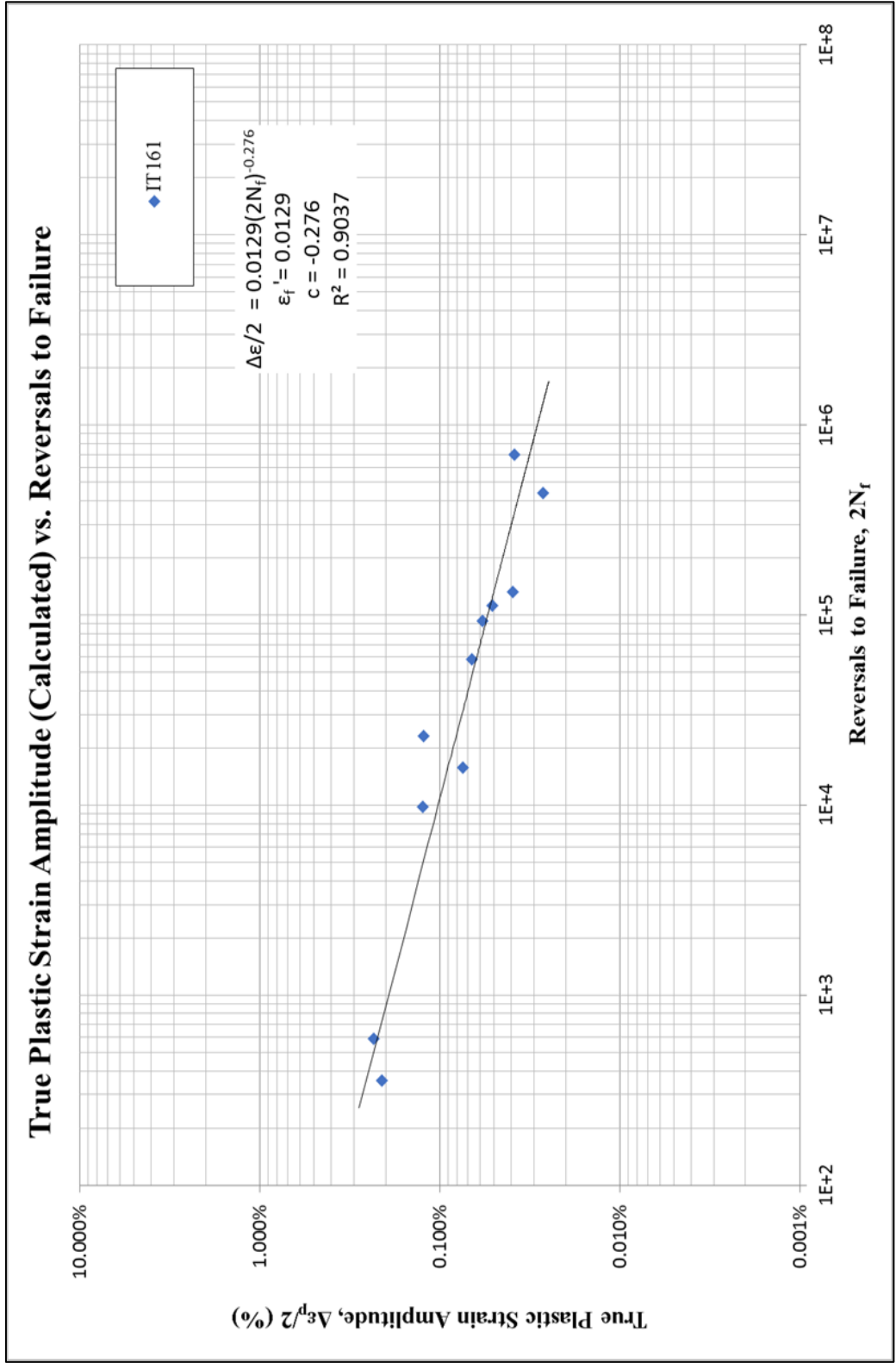


Figure 10: True plastic strain amplitude (calculated) versus reversals to failure

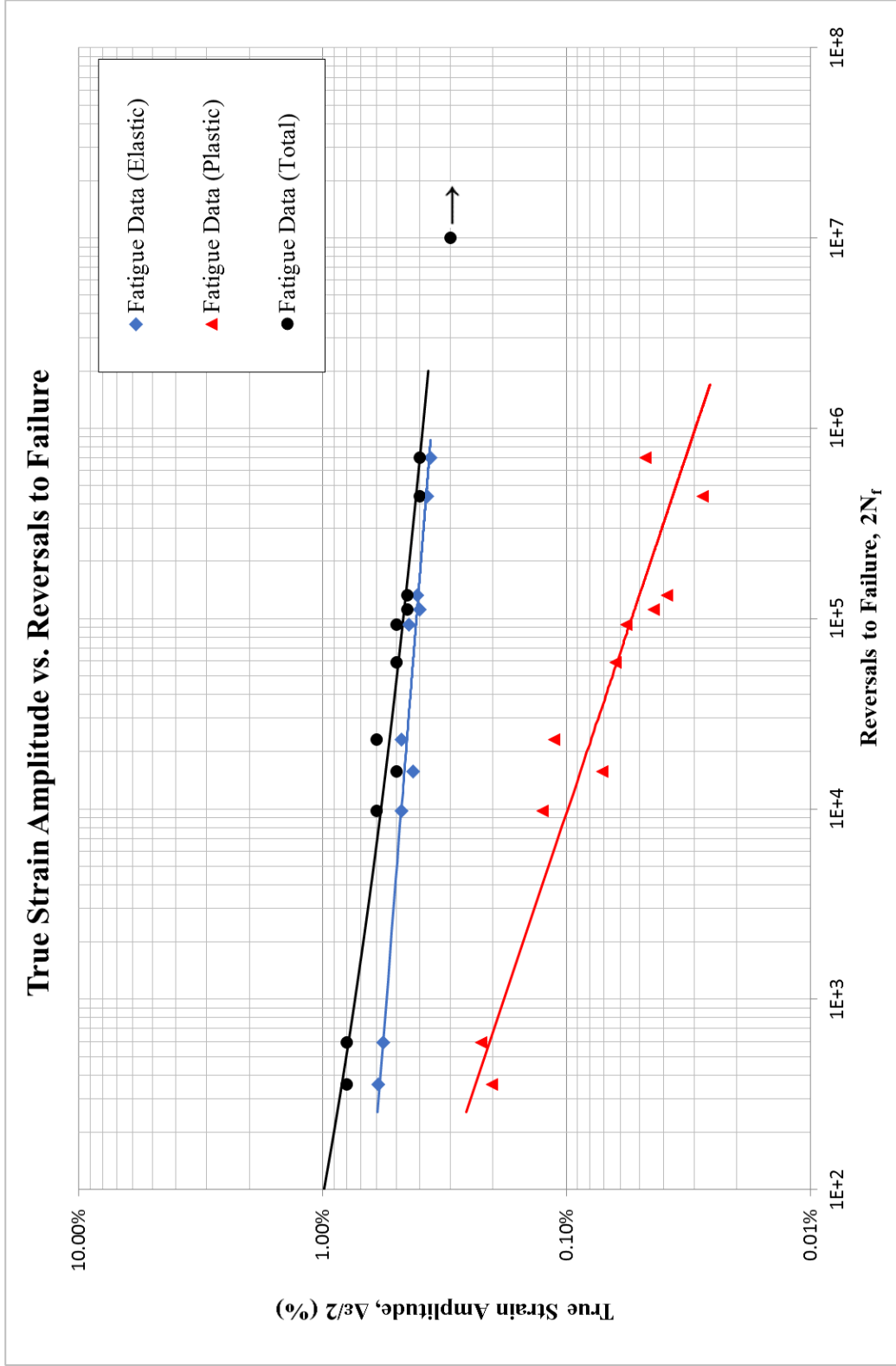


Figure 11: True strain amplitude versus reversals to failure

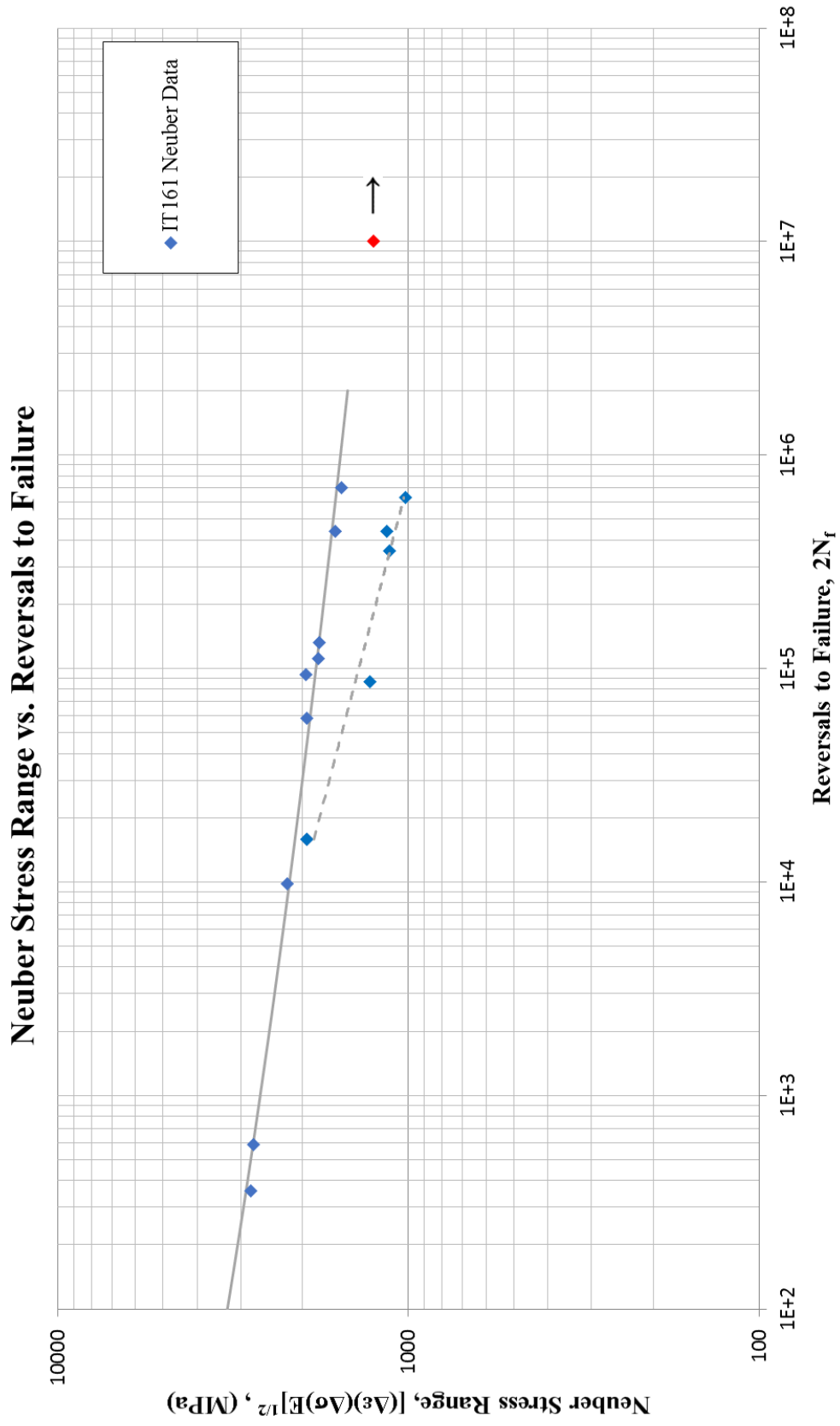


Figure 12: Neuber stress range versus reversals to failure

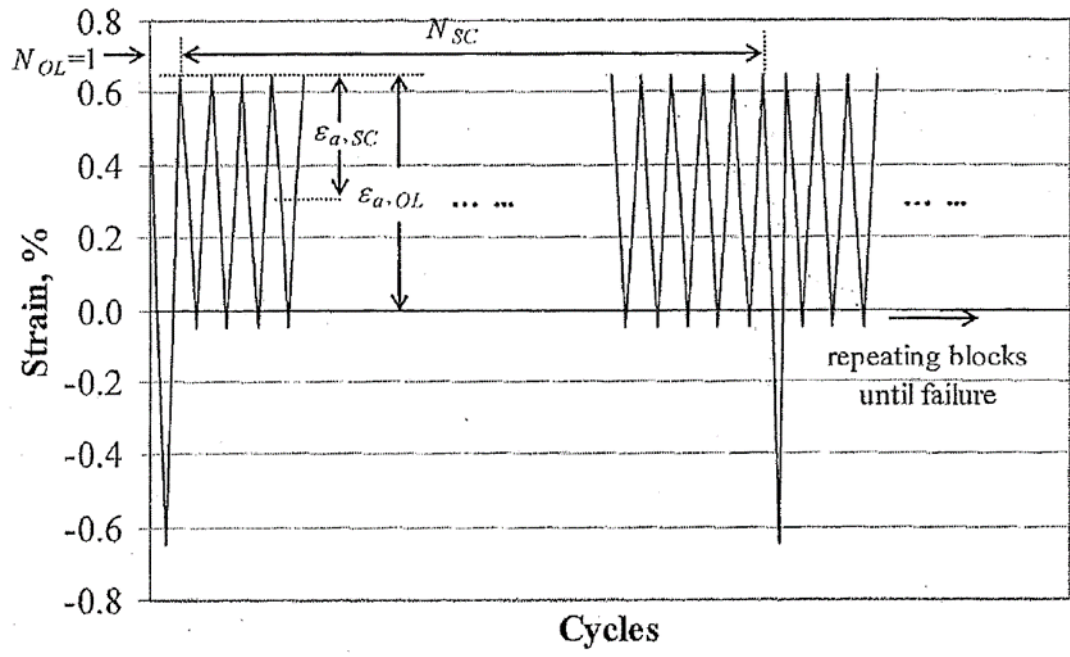


Figure 13: Periodic overload history

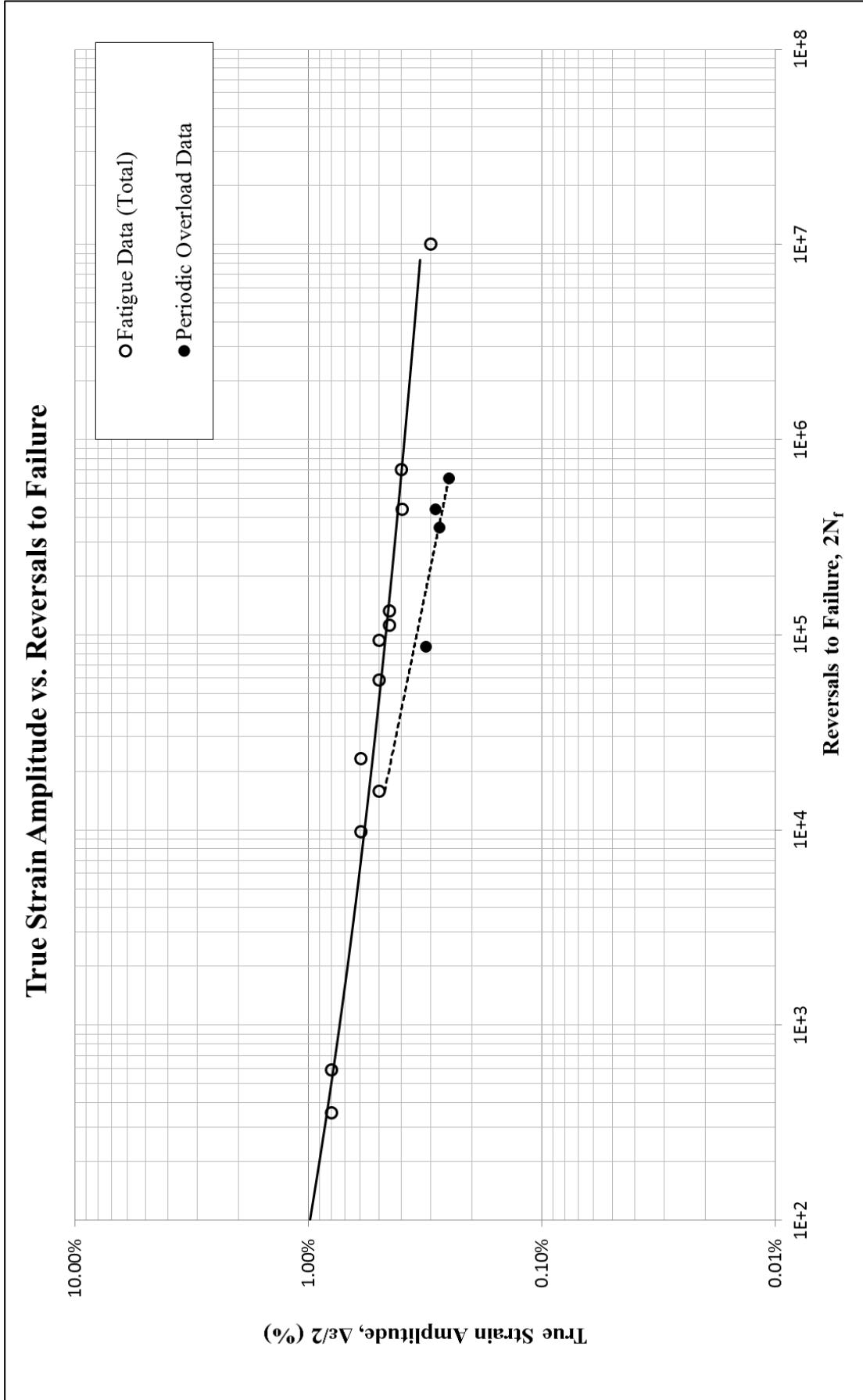


Figure 14: Periodic overload data superimposed with constant amplitude fatigue data





## REFERENCES

- [1] ASTM E606/E606M-12 Standard Test Method for Strain-Controlled Fatigue Testing, ASTM International, West Conshohocken, PA, 2012
- [2] ASTM E83-10a Standard Practice for Verification and Classification of Extensometer Systems, ASTM International, West Conshohocken, PA, 2010
- [3] ASTM E1012-14 Standard Practice for Verification of Testing Frame and Specimen Alignment Under Tensile and Compressive Axial Force Application, ASTM International, West Conshohocken, PA, 2014,
- [4] ASTM E8/E8M-15a Standard Test Methods for Tension Testing of Metallic Materials, ASTM International, West Conshohocken, PA, 2015
- [5] ASTM E739-10 Standard Practice for Statistical Analysis of Linear or Linearized Stress-Life (S-N) and Strain-Life ( $\epsilon$ -N) Fatigue Data, ASTM International, West Conshohocken, PA, 2010
- [6] ASTM E646-07 Standard Test Method for Tensile Strain-Hardening Exponents (n - Values) of Metallic Sheet Materials, ASTM International, West Conshohocken, PA, 2007
- [7] Stephens R. I., Fatemi A., Stephens R.R. and Fuchs H. O., “*Metal Fatigue in Engineering*”, Second edition, Wiley Interscience, 2000

# APPENDIX A

**Table A.1: Summary of monotonic tensile test results**

Specimen ID	D <sub>0</sub> , mm	D <sub>f</sub> , mm	R, mm	L <sub>0</sub> , mm	L <sub>f</sub> , mm	E, GPa	YS, MPa	S <sub>u</sub> , MPa	K, MPa	n	%EL	%RA	ε <sub>f</sub> , %	σ <sub>f</sub> , MPa
1	5.08	5.01	1.207	7.62	7.83	208.03	996.28	1200.89	4025.3	0.2256	2.79%	2.47%	2.77%	750.48
2	5.08	5.01	1.207	7.62	7.84	205.24	1037.78	1163.81	4738.4	0.2449	2.83%	2.47%	2.77%	712.33
Avg.	5.08	5.01	1.207	7.62	7.84	206.64	1017.03	1182.35	4381.9	0.2353	2.81%	2.47%	2.77%	731.41

**Table A.2: Summary of constant amplitude completely reversed fatigue test results**

Specimen ID	Applied Strain %	Test control mode	Test freq., Hz	E, GPa [e]	At midlife (N <sub>50%</sub> )							(2N <sub>f</sub> ) <sub>10%</sub> , [b] reversals	(2N <sub>f</sub> ) <sub>50%</sub> , [c] reversals	Failure location [d]
					E', GPa	Δε/2, %	Δε <sub>p</sub> /2, (calculated) %	Δε <sub>p</sub> /2, (measured) %	Δσ/2, MPa	σ <sub>m</sub> , MPa	2N <sub>50%</sub> , [a] reversals			
12	±0.80	strain	0.3	205.9	202.0	0.799%	0.234%	0.223%	1162.8	-91.5	295	-	590	IGL
14	±0.80	strain	0.3	205.0	202.7	0.799%	0.209%	0.203%	1208.9	-129.6	178	162	356	IGL
6	±0.60	strain	0.3	207.6	208.4	0.600%	0.124%	0.126%	986.8	-78.4	4,880	9,330	9,760	IGL
10	±0.60	strain	0.3	210.3	205.5	0.599%	0.123%	0.112%	1001.3	-95.4	11,590	17,180	23,180	IGL
1	±0.50	strain	1	208.0	207.7	0.499%	0.058%	0.057%	918.6	-204.0	46,640	60,532	93,280	IGL
2	±0.50	strain	1	211.7	210.2	0.499%	0.075%	0.072%	898.6	-20.0	7,898	8,000	15,796	IGL
16	±0.50	strain	10	209.1	207.2	0.499%	0.067%	0.063%	904.7	-93.0	29,355	-	58,710	IGL
8	±0.45	strain	10	212.5	208.6	0.450%	0.051%	0.044%	847.4	-38.4	55,825	-	111,650	IGL
15	±0.45	strain	10	209.3	209.0	0.450%	0.039%	0.039%	858.9	-78.0	66,364	-	132,728	IGL
7	±0.40	strain	10	209.8	210.3	0.399%	0.027%	0.028%	781.1	-68.0	218,842	-	437,684	KE
9	±0.40	strain	10	204.3	209.4	0.399%	0.038%	0.047%	737.2	-58.5	350,432	-	700,864	IGL
17	±0.30	strain	20	211.0	210.0	0.298%	0.002%	0.001%	624.5	-0.9	-	-	>10,000,000	No Failure
24	±0.30	strain	20	209.0	208.0	0.298%	0.001%	0.000%	612.5	-1.3	-	-	>10,000,000	No Failure

[a] 2N<sub>50%</sub> is defined as the midlife reversal;

[b] (2N<sub>f</sub>)<sub>10%</sub> is defined as reversal of 10% load drop;

[c] (2N<sub>f</sub>)<sub>50%</sub> is defined as reversal of 50% load drop or failure;

[d] IGL = Inside gage length

[e] E value was calculated from the first cycle.

**Table A.3: Measurement of Specimen Dimensions**

Specimen ID	Total Length (mm)	Grip Diameter* (mm)	Grip Length* (mm)	Gage Diameter (mm)	Gage Length (mm)
161_1	108.05	12.56/12.55	37.58/37.57	5.08	7.62
161_2	108.09	12.55/12.54	37.52/37.89	5.08	7.62
161_3	108.01	12.54	37.56	5.09	7.62
161_4	108.07	12.52/12.53	37.32/37.79	5.08	7.62
161_6	107.96	12.54/12.55	37.72/37.70	5.08	7.62
161_7	108.06	12.54	37.56/38.71	5.08	7.62
161_8	108.04	12.54/12.55	37.36/37.55	5.08	7.62
161_9	108.05	12.55	37.47/37.85	5.08	7.62
161_10	108.05	12.55/12.57	37.88/37.87	5.08	7.62
161_12	108.06	12.55	37.58/37.78	5.08	7.62
161_14	108.16	12.52/12.54	37.91/37.73	5.08	7.62
161_15	108.03	12.54	37.66/37.76	5.08	7.62
161_16	108.02	12.54/12.56	37.74/37.72	5.08	7.62
161_17	108.03	12.54/12.56	37.88/37.58	5.08	7.62
161_18	108.06	12.54	37.46/37.75	5.08	7.62
161_19	108.03	12.56	37.76/37.74	5.08	7.62
161_20	108.03	12.55	37.87/37.52	5.08	7.62
161_21	108.03	12.56	37.82/37.59	5.08	7.62
161_22	108.01	12.54	37.70/37.71	5.08	7.62
161_23	108.02	12.55	37.84/37.83	5.08	7.62
161_24	108.03	12.54	37.36/37.72	5.08	7.62
161_25	108.04	12.55	37.85/37.84	5.08	7.62

**Table A.4: Summary of periodic overload fatigue test results**

Spec. ID	Test Control mode	Test Freq. OL/SC (Hz)	E (GPa) [a]	Load History Description											Exp.Life (Blks)	N <sub>f,SC(eq)</sub> (Cycles)	OL Damage Ratio	Failure Location [b]
				$\epsilon_{a,SC}$ (%)	$\epsilon_{m,SC}$ (%)	$\Delta\epsilon_p/2,SC$ (calculated) (%)	$\sigma_{a,SC}$ (MPa)	$\sigma_{m,SC}$ (MPa)	N <sub>sc</sub> (Cycles)	$\epsilon_{a,OL}$ (%)	$\Delta\epsilon_p/2,OL$ (calculated) (%)	$\sigma_{a,OL}$ (MPa)	$\sigma_{m,OL}$ (MPa)	N <sub>f,OL</sub> (Cycles)				
19	Strain	1 4	210.6	0.315%	0.225%	0.020%	621.1	196.4	100	0.539%	0.082%	962.3	-132.8	10000	413	43522	0.0413	IGL
18	Strain	1 4	206.6	0.285%	0.250%	0.013%	561.8	202.3	100	0.533%	0.089%	917.1	-135.8	10000	1805	220256	0.1805	IGL
20	Strain	1 4	210.8	0.275%	0.265%	0.012%	554.7	230.3	100	0.537%	0.094%	934.9	-123.2	10000	1509	177730	0.1509	IGL
21	Strain	1 4	207.3	0.250%	0.290%	0.008%	500.8	269.9	100	0.538%	0.081%	948.9	-162.3	10000	2410	317523	0.241	IGL

[a] E value was calculated from the first cycle;

[b] IGL = Inside gage length, KE = At knife edge.

All stress values reported are from midlife.

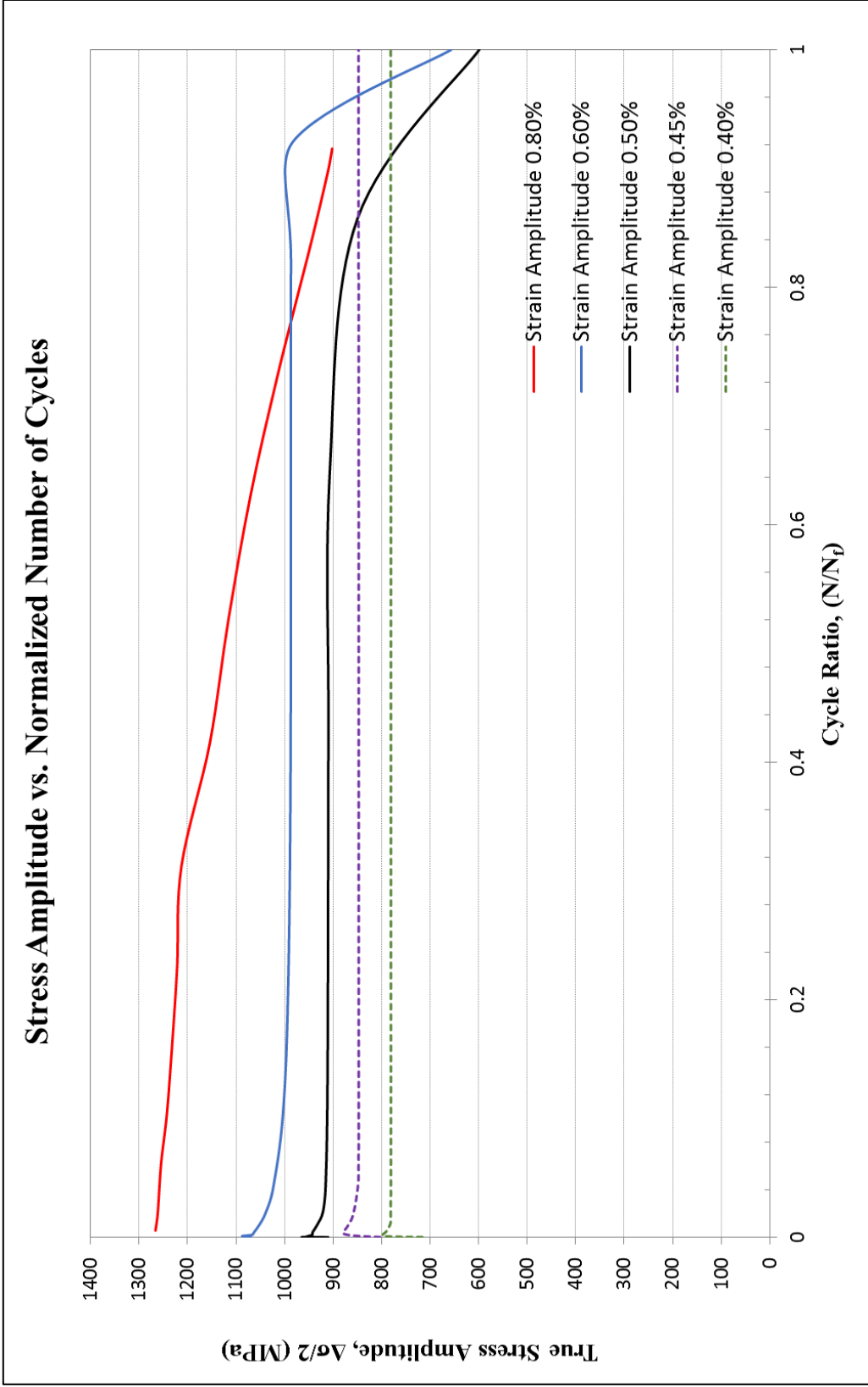


Figure A.1a: True stress amplitude versus normalized number of cycles

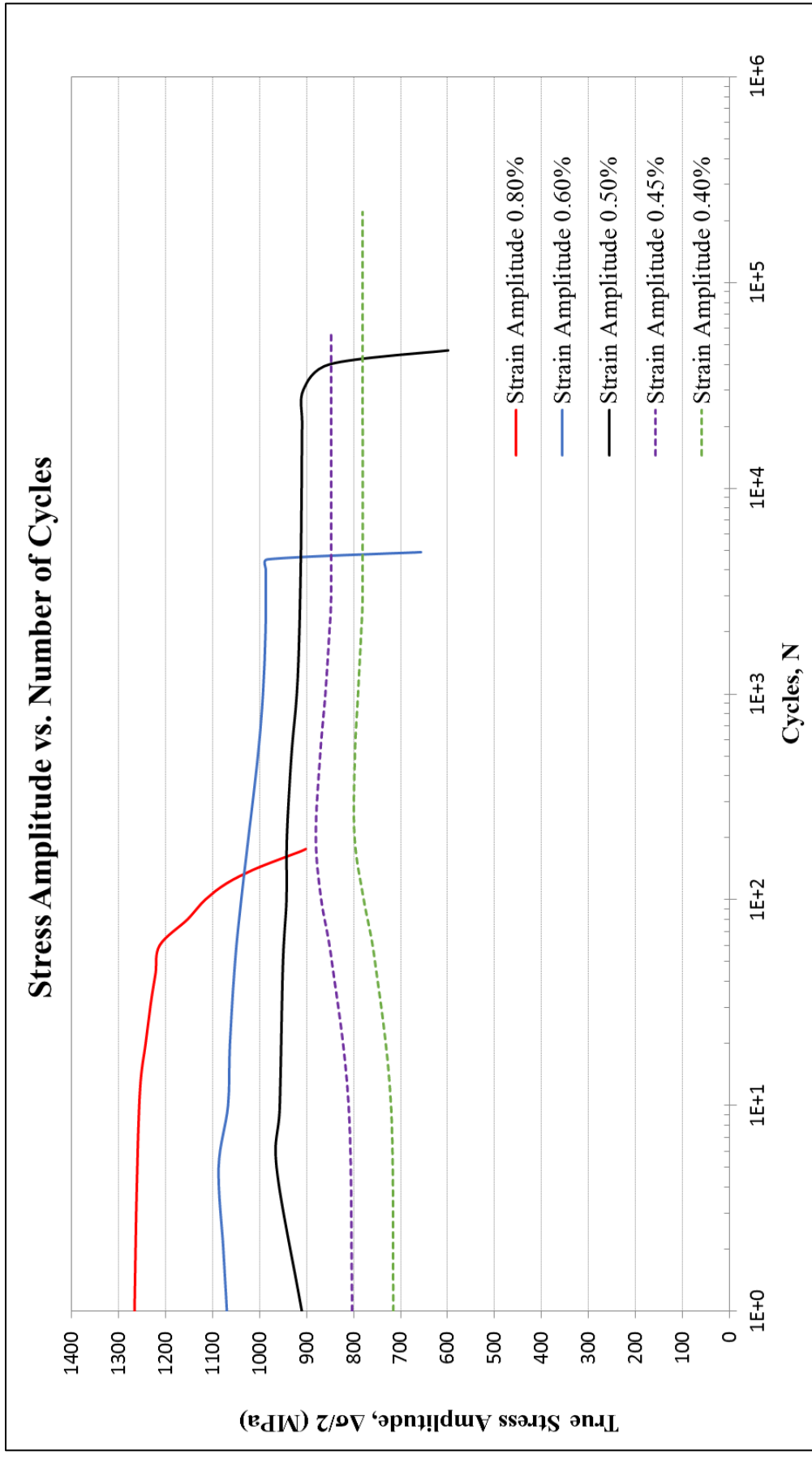


Figure A.1b: True stress amplitude versus number of cycles



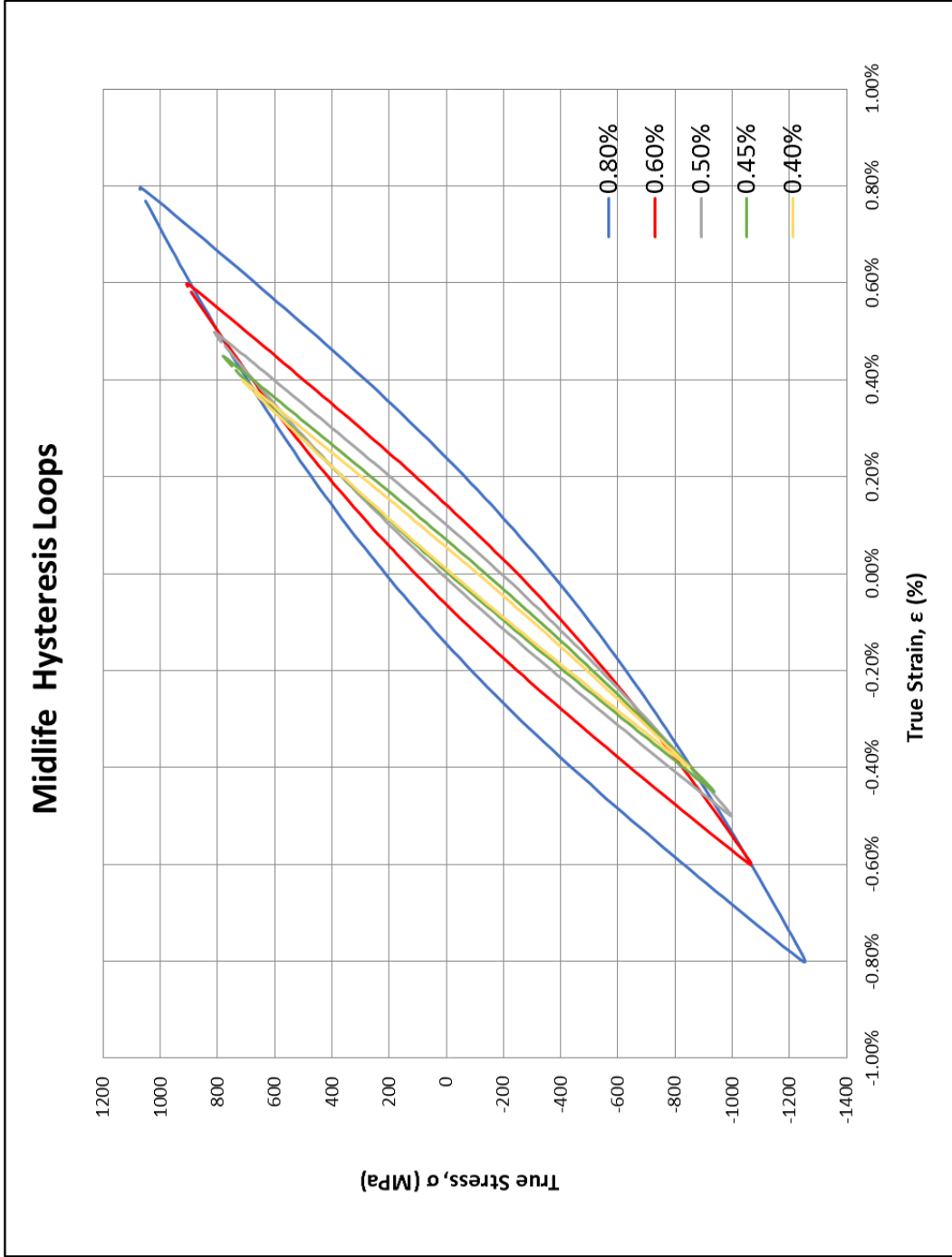


Figure A.2: Composite plot of midlife hysteresis loops

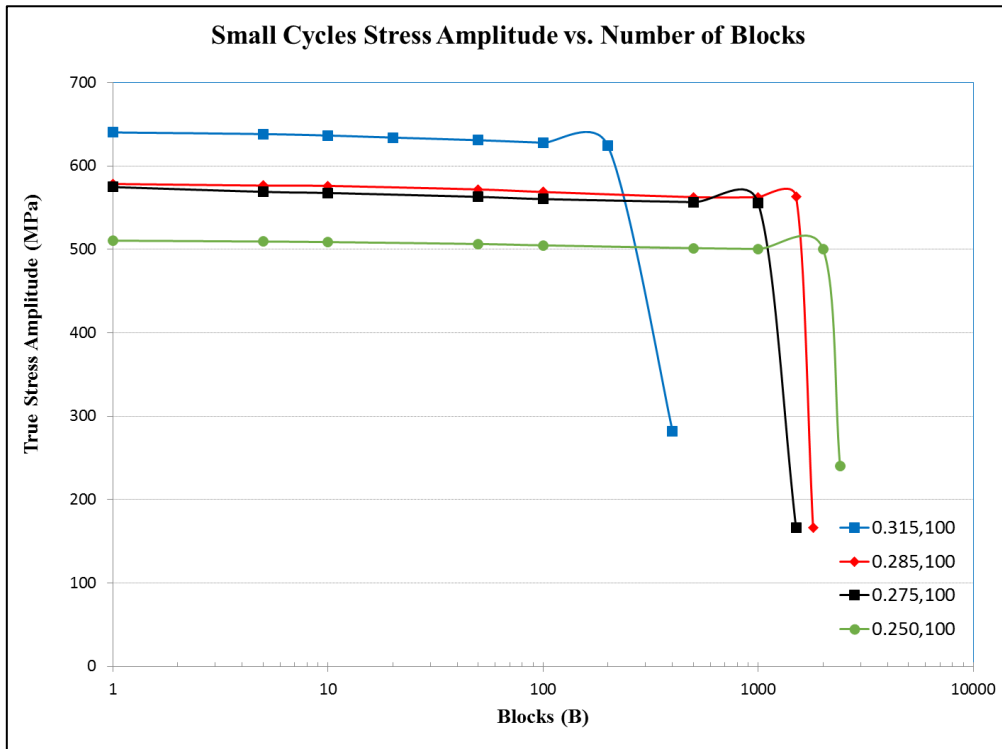


Figure A.3a: Small cycle amplitude transient response throughout the life

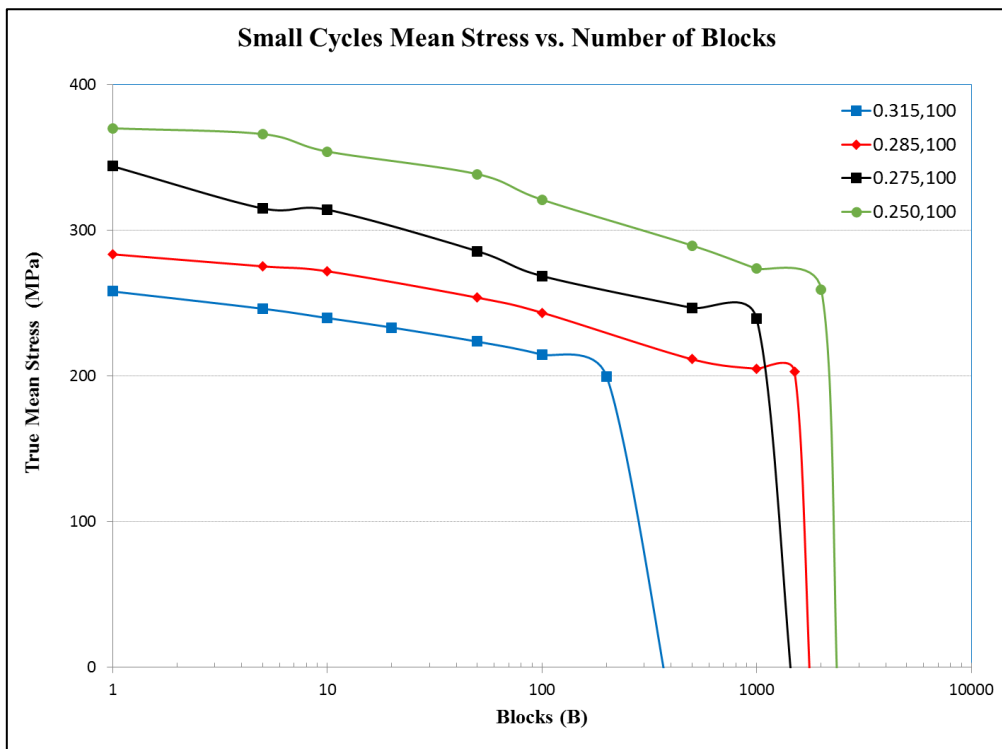


Figure A.3b: Small cycle mean transient response throughout the life

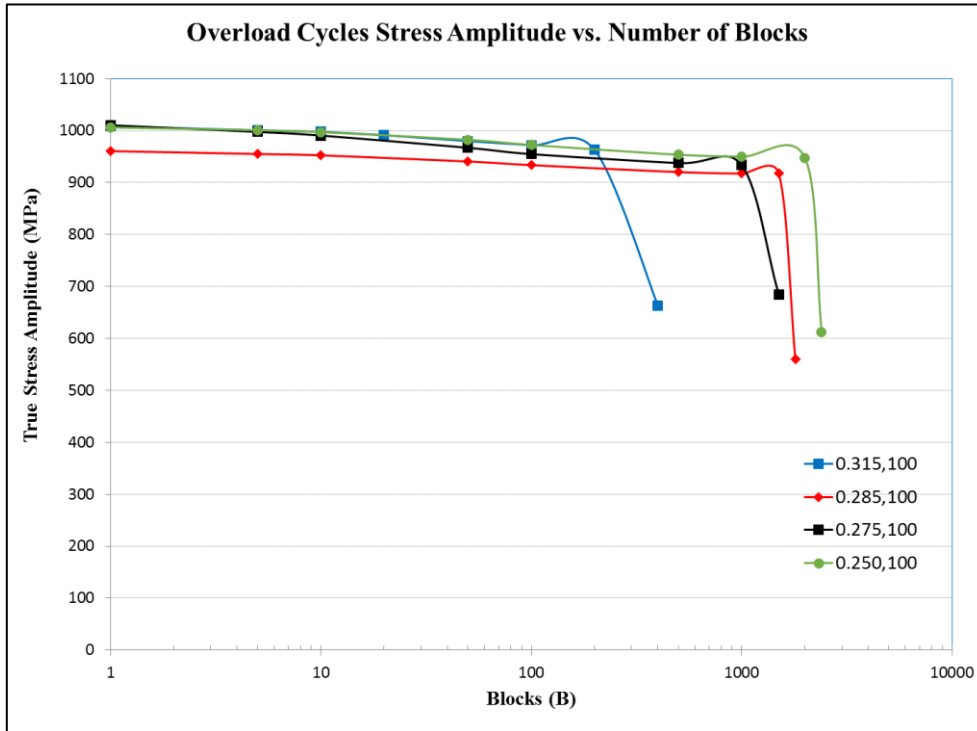


Figure A.4a: Overload cycle amplitude transient response throughout the life

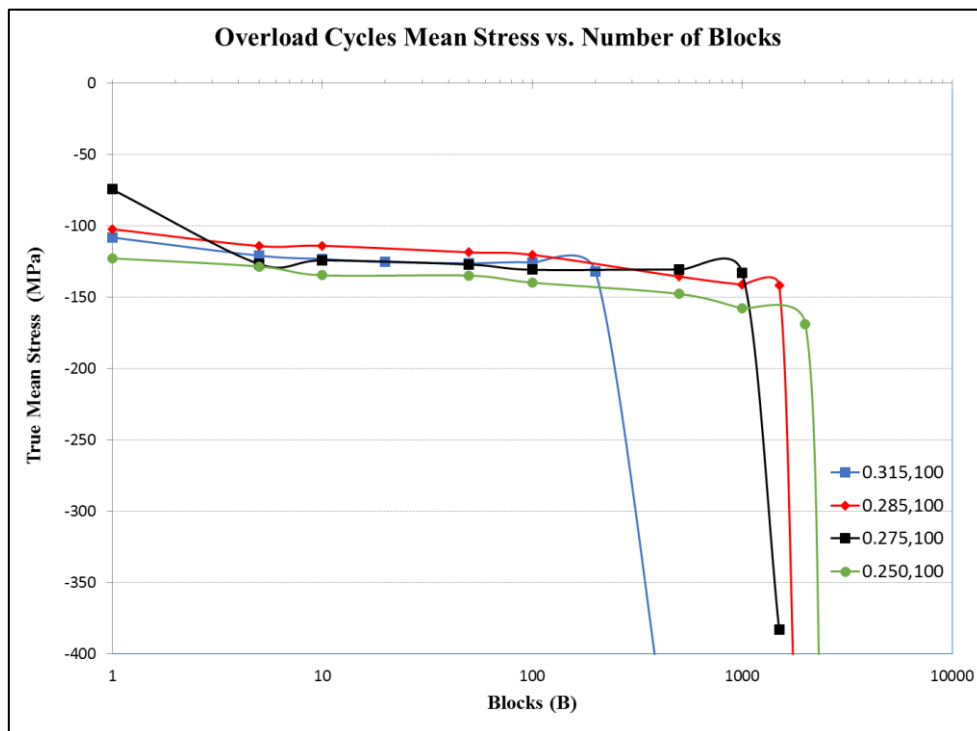


Figure A.4b: Overload cycle mean transient response throughout the life

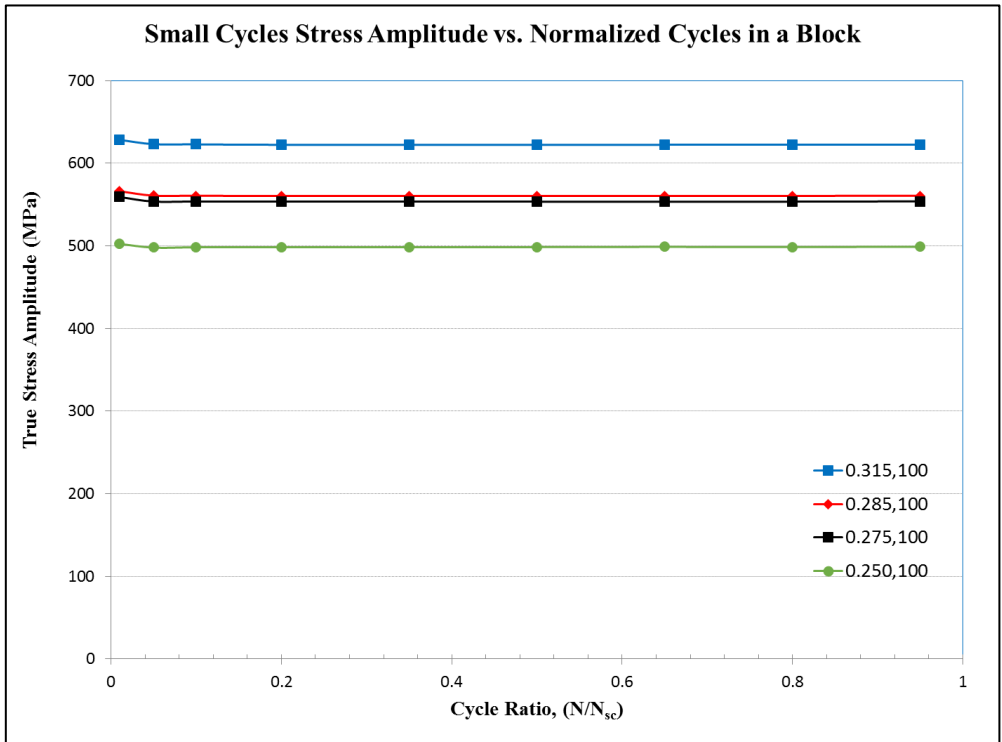


Figure A.5a: Small cycle transient response amplitude throughout one load block at midlife

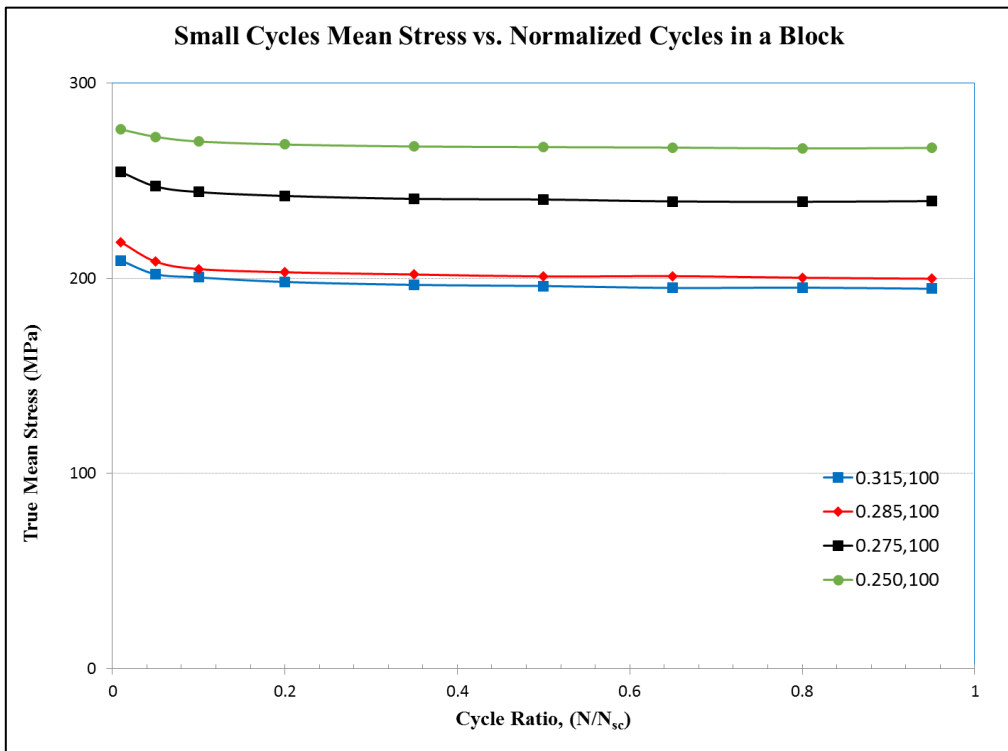
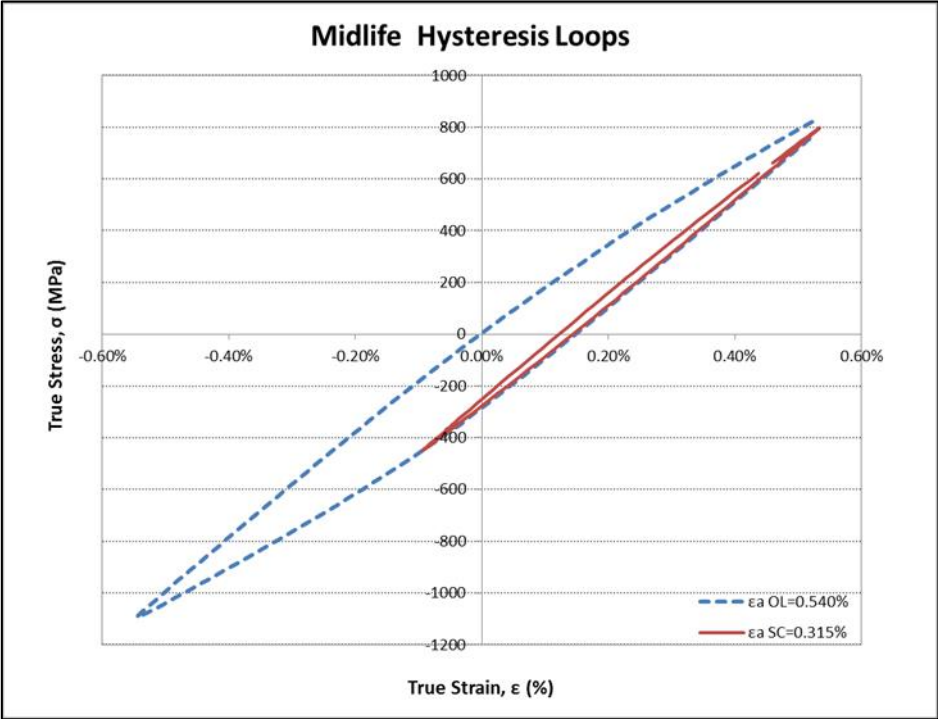
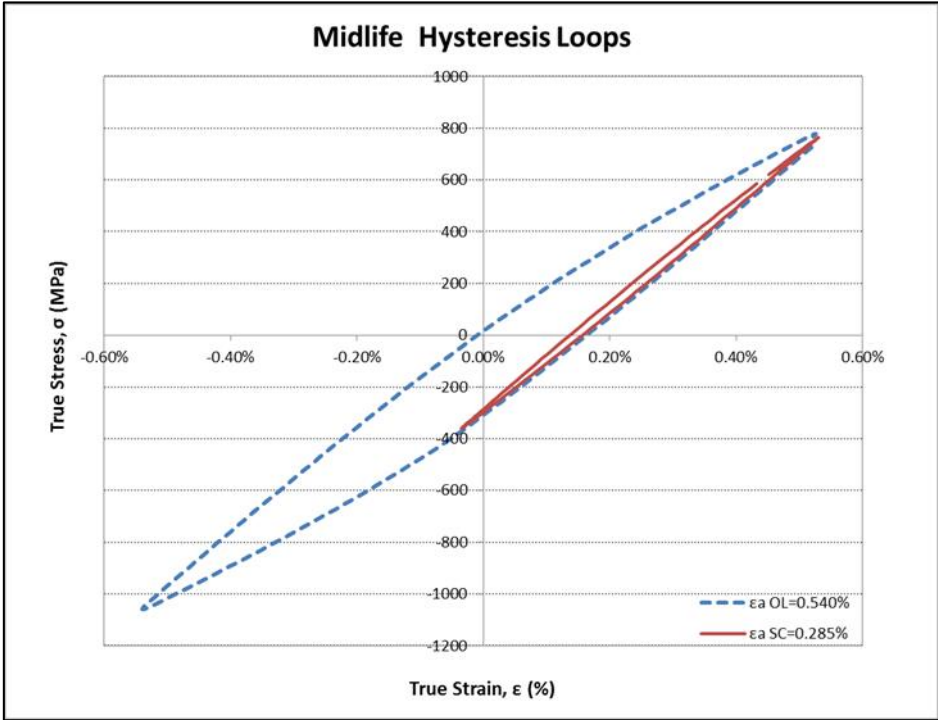


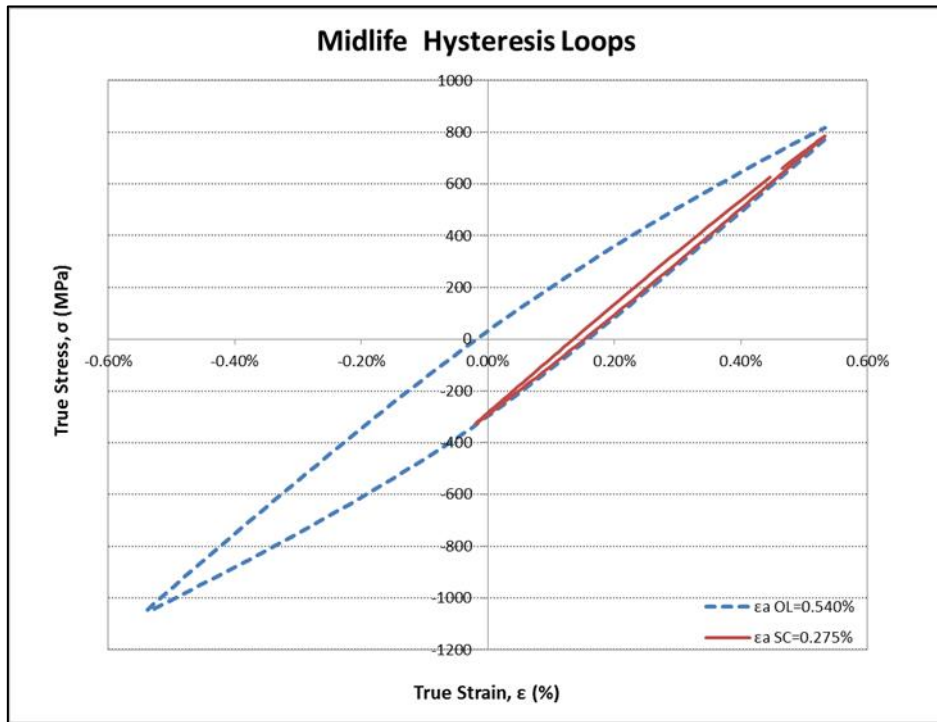
Figure A.5b: Small cycle transient response mean throughout one load block at midlife



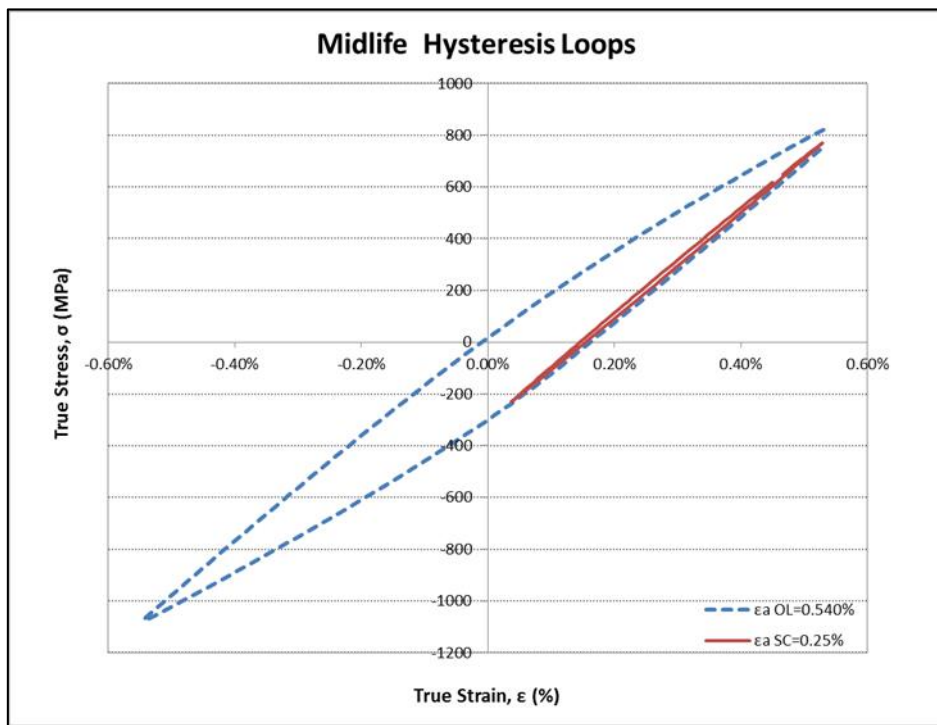
(a)



(b)



(c)



(d)

Figure A.6(a-d): Periodic overload midlife hysteresis loop superimposed with small cycle midlife hysteresis loop

## **APPENDIX B**

### **Rockwell Hardness Test**

The Rockwell hardness number HR is determined by the difference in depth of penetration resulting from the application of an initial minor load followed by a larger major load.

A Rocky test machine was applied to get the Rockwell Hardness. Indenters include spherical and hardened steel balls and a conical diamond (Brale) indenter, which is used for the hardest materials. The 1/16-in. ball indenter was used for HRB scale, the diamond indenter was used for HRC scale. For the material of this project, we use HRC to describe the hardness. Here in this study, two specimens were applied for hardness testing. Five different locations from each grip end surface were chosen for testing, and two locations in gauge area were tested. The results are shown in Table B.1 and Table B.2.

Take the average value, the hardness of this material in gauge and grip area is 34.7 HRC and 24. HRC, respectively.

**Table B.1: Rockwell Hardness (HRC) in grip area**

Specimen ID	Data #1	Data #2	Data #3	Data #4	Data #5	AVG
IT161_17	25.9	25.8	24.2	25.0	26.0	<b>25.4</b>
IT161_24	25.8	24.2	23.2	24.1	24.7	<b>24.4</b>

**Table B.2: Rockwell Hardness (HRC) in gauge area**

Specimen ID	Data #1	Data #2	AVG
IT161_17	34.6	34.6	<b>34.6</b>
IT161_24	34.0	35.5	<b>34.8</b>



## **APPENDIX C**

## Fracture Surface Examination



Figure C.1: Fracture surface of specimen #6 under 0.6% strain amplitude (fails with 9760 reversals )



Figure C.2: Fracture surface of specimen #16 under 0.5% strain amplitude (fails with 58710 reversals )





Figure C.3: Fracture surface of specimen #15 under 0.45% strain amplitude (fails with 132728 reversals )



Figure C.4: Fracture surface of specimen #18 under overload